

## Pyroptosis

How to cite: *Angew. Chem. Int. Ed.* **2021**, *60*, 8018–8034

International Edition: doi.org/10.1002/anie.202010281

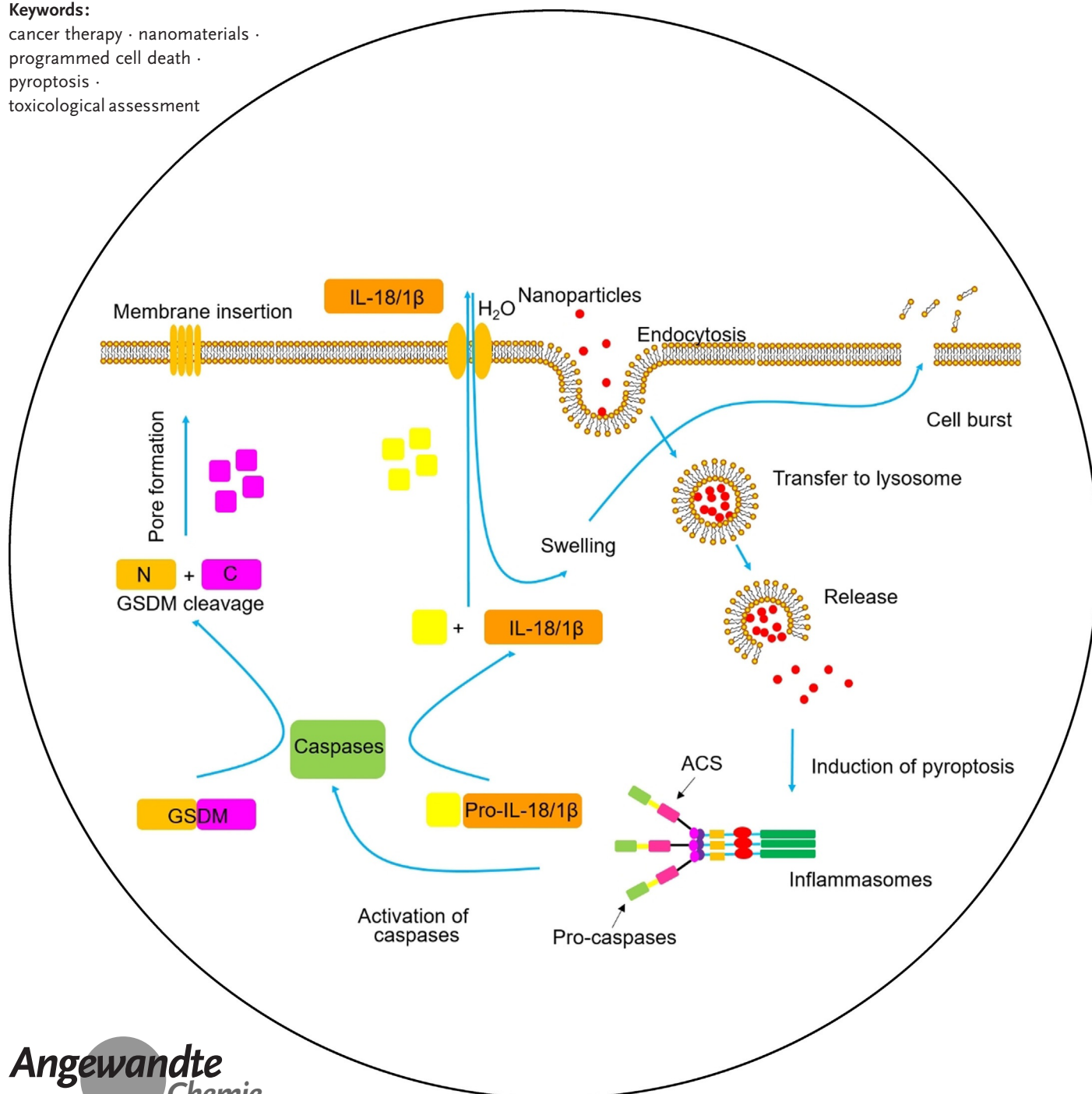
German Edition: doi.org/10.1002/ange.202010281

# Cell Death Mediated by the Pyroptosis Pathway with the Aid of Nanotechnology: Prospects for Cancer Therapy

Dan Wu,\* Sheng Wang,\* Guocan Yu,\* and Xiaoyuan Chen\*

**Keywords:**

cancer therapy · nanomaterials · programmed cell death · pyroptosis · toxicological assessment



**P**yroptosis, a unique form of programmed cell death (PCD) that is characterized by DNA fragmentation, chromatin condensation, cellular swelling with big bubbles, and leakage of cell content, has been proven to have a close relationship with human diseases, such as inflammatory diseases and malignant tumors. Since a new gasdermin-D (GSDMD) protein was identified in 2015, various strategies have been developed to induce pyroptosis for cancer therapy, including ions, small-molecule drugs and nanomaterials. Although there are a number of reviews about the close relationship between the pyroptosis mechanism and the occurrence of various cancers, a summary covering recent progress in the field of nanomedicines in pyroptosis-based cancer therapy has not yet been presented. Therefore, it is urgent to fill this gap and light up future directions for the use of this powerful tool to combat cancer. In this Minireview, recent progress in cancer treatment based on pyroptosis induced by nanoparticles will be described in detail, the design highlights and the therapeutic advantages are emphasized, and future perspectives in this emerging area are proposed.

## 1. Introduction

As a result of a series of genetic variations, normal cells are transformed into malignant cells with the ability to avoid cell death, thus leading to tumor development. The imbalance between cell death and cell proliferation causes the number of tumor cells to increase rapidly. Although there have been considerable therapeutic advancements, cancer is still the second major cause of death in the world after cardiovascular diseases. According to the World Health Organization (WHO), cancer deaths will rise by as much as 80% by 2030.<sup>[1]</sup> One of the critical issues in cancer treatment is how to effectively kill cancer cells while leaving healthy cells intact. A significant therapeutic method for the killing of cancer cells is the promotion of apoptotic cell death. Nevertheless, the efficiency of apoptosis induction is sometimes limited in tumors owing to the intrinsic or acquired resistance of cancer cells to apoptosis.<sup>[2]</sup> Therefore, it is necessary to explore additional cell death modes for effective cancer treatment.

Cells can undergo diverse types of death. Previously, apoptosis was regarded as the only form of programmed cell death (PCD).<sup>[3]</sup> However, recent studies have proven two other unidentified forms of PCD, namely ferroptosis and pyroptosis. Unlike apoptosis, ferroptosis is a cell death which relies on reactive oxygen species (ROS) and iron. Owing to the high degree of membrane lipid peroxidation and the existence of oxidative stress, plasma membranes lack selective permeability, which leads to cytological changes including smaller mitochondria, vanishing or decreased mitochondria cristae, and a shrinking mitochondrial membrane.<sup>[4]</sup> Ferroptosis is being increasingly recognized as an adaptive characteristic to clear malignant cells and has been utilized for cancer therapy. Pyroptosis is another unique form of PCD and was first discovered in myeloid cells infected by bacteria or pathogens in 1992.<sup>[5]</sup> Later, Zychlinsky discovered that

*Shigella dysenteriae* was able to activate caspase-1 in host cells, and Boise et al. put forward the term pyroptosis to distinguish this death mode that is totally different from apoptosis.<sup>[6]</sup> After that, there were a plethora of studies related to pyroptosis, while its mechanism remained unknown. In 2015, Shao et al. discovered and identified a new gasdermin-D (GSDMD) protein, which is kept in an auto-inhibition state under normal circumstances. After caspase cutting, GSDMD releases gasdermin-N and gasdermin-C domains in which the gasdermin-N domains combine membrane phospholipids and perforate cell membranes with a pore size of circa 18 nm, disrupting the osmotic potential and leading to cell swelling with big bubbles.<sup>[7]</sup> Apart from GSDMD, other members of the gasdermin family including GSDMA, GSDMB, GSDMC, deafness autosomal dominant 5 (DFNA5)/GSDME, and

DFNB59 also possess the ability to perforate membranes and are able to activate pyroptosis.<sup>[8]</sup> It has been proven that there is a close relationship between various human diseases and pyroptosis, particularly inflammatory diseases and malignant tumors.<sup>[9]</sup> Although pyroptosis is often detrimental to normal organs and tissues,<sup>[10]</sup> it can be favorable to cancer treatment by specifically activating PCD at the sites of action. Induction of pyroptotic death by various stimuli can effectively eliminate malignant cells and provide new strategies for cancer therapy.<sup>[11]</sup>

---

[\*] Dr. D. Wu  
College of Materials Science and Engineering  
Zhejiang University of Technology  
Hangzhou, 310014 (P. R. China)  
E-mail: danwu@zjut.edu.cn

Dr. S. Wang  
School of Life Sciences, Tianjin University and Tianjin Engineering  
Center of Micro-Nano Biomaterials and Detection-Treatment Technology  
Tianjin 300072 (P. R. China)  
E-mail: shengwang@tju.edu.cn

Dr. G. Yu, Prof. Dr. X. Chen  
Laboratory of Molecular Imaging and Nanomedicine  
National Institute of Biomedical Imaging and Bioengineering  
National Institutes of Health  
Bethesda, Maryland, 20892 (USA)

Prof. Dr. X. Chen  
Yong Loo Lin School of Medicine and Faculty of Engineering  
National University of Singapore  
Singapore, 117597  
(Singapore)  
E-mail: guocan.yu@nih.gov  
chen9647@gmail.com

 The ORCID identification number(s) for the author(s) of this article can be found under:  
<https://doi.org/10.1002/anie.202010281>.

Morphologically, pyroptosis is in line with the features of both apoptosis and necrosis. At the early stage, pyroptosis leads to apoptosis-like DNA fragmentation and chromatin condensation, followed by necrosis-like characteristics, such as the formation of transmembrane pores, cellular swelling with big bubbles, and cell membrane breakage, which causes the release of inflammation molecules (Interleukin-1 $\beta$ , IL-1 $\beta$ , and IL-18) and cell contents (Scheme 1).<sup>[12]</sup> In the canonical pathway, pattern recognition receptors (PRRs) first recognize damage-associated molecular patterns (DAMPs) or pathogen-associated molecular patterns (PAMPs) and then initiate pyroptosis. PRRs related to pyroptosis mainly include absent in melanoma 2 (AIM2)-like receptors (ALRs), toll-like receptors (TLRs), and intracellular nucleotide-binding oligomerization domain (NOD)-like receptors (NLRs). PRRs recognize different DAMPs or PAMPs to form specific inflammasomes. For example, viruses, bacteria, fungi, ATP, and uric acid can initiate NLRP3 inflammasomes,<sup>[13]</sup> while type III secretory system proteins and flagellin can induce NLRC4 inflammasomes,<sup>[14]</sup> and double-stranded DNA existing in viruses or bacteria can promote the formation of AIM2 inflammasomes.<sup>[15]</sup> In response to DAMPs and PAMPs, pro-caspase-1 is simultaneously recruited to form inflammasomes, which also contain adaptor protein apoptosis-associated speck like proteins (ASC). Linkage between pro-caspase-1 and ASC is attributed to the caspase activation and recruitment domain (CARD) of ASC interactions with pro-caspase-1.<sup>[16]</sup> Caspase-1 is not only able to regulate the active process of IL-1 $\beta$  and IL-18 but can also cut GSDMD into two fragments: C-terminal domain and N-terminal domain. The necrotic N-terminal domains translocate into the plasma membrane and form cell membrane pores. These pores

facilitate the exchange between the external and internal sides of the cell membrane, and the cellular osmotic pressure is rapidly disrupted. Owing to a significant quantity of water entering the cell, cells swell with large bubbles and eventually die, permitting the cell contents and inflammatory cytokines to escape extracellularly.<sup>[17]</sup> In the non-canonical pathway, cytoplasmic lipopolysaccharide (LPS) directly mediates the pyroptosis process triggered by caspase-4/5 (human) and caspase-11 (mice). Similar to the canonical pathway, active caspase-4/5/11 can also cut GSDMD into N-terminal domains and C-terminal domains, which causes the generation of membrane pores.<sup>[18]</sup> Activated caspase-4/5/11 is capable of interacting with caspase-1 to induce its activation in the presence of ASC and NLRP3. It is worth noting that caspase-4/5/11 is not involved in pro-IL-1 $\beta$  and pro-IL-18. Nevertheless, in an NLRP3 inflammasome-involving manner, activated caspase-11 could indeed induce the secretion of a small quantity of IL-1 $\beta$ . Recent studies have demonstrated that, in addition to canonical and non-canonical pathways, pyroptosis can also be initiated by other caspases. In normal and cancer cells which express high levels of GSDME, chemotherapy drugs can activate caspase-3 and then cleave GSDME to generate N-terminal domains, which subsequently form transmembrane pores, eventually resulting in pyroptosis. Meanwhile, inhibition of transforming growth factor- $\beta$  (TGF- $\beta$ )-activated kinase 1 (TAK1) by Yersinia effector protein YopJ or small-molecule inhibitors inducing caspase-8, which involves the cleavage of GSDMD, can also lead to pyroptotic cell death.

There are several studies revealing that certain ions, molecules or chemotherapeutic drugs, such as iron,<sup>[19]</sup> metformin,<sup>[20]</sup> docosahexaenoic acid (DHA),<sup>[21]</sup> cisplatin,<sup>[22]</sup> pa-



Dan Wu was born in Henan, China, in 1988. She received her Ph.D. degree from Zhejiang University in 2016 under the supervision of Prof. Guping Tang. She is currently a lecturer at the college of materials science and engineering at Zhejiang University of Technology. Her current research interests are focused on the construction of functional biomaterials.



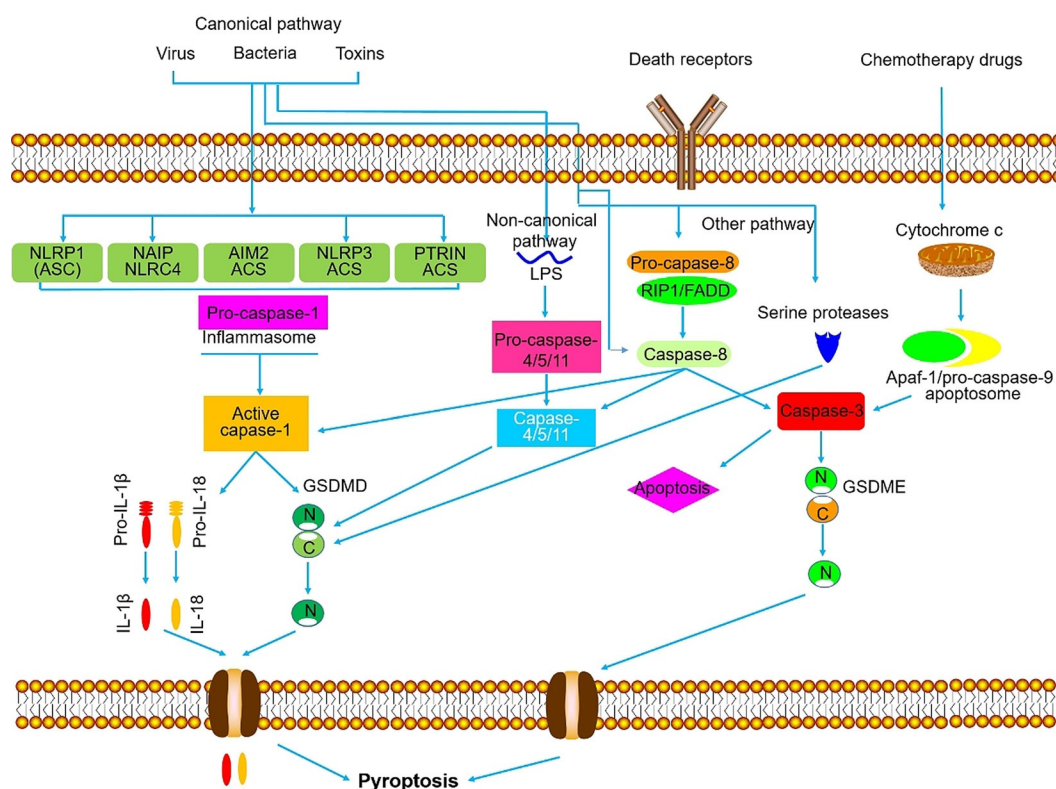
Guocan Yu received his Ph.D. degree from Zhejiang University in 2015 under the supervision of Prof. Feihe Huang. He then worked for five years as a postdoctoral researcher in Prof. Xiaoyuan (Shawn) Chen's research group at the National Institutes of Health (NIH). His research interests are focused on the construction of functional supramolecular theranostics and stimuli-responsive biomaterials.



Sheng Wang received his Ph.D. in Materials Science and Engineering from Tianjin University in 2015 under the supervision of Prof. Jin Chang. He then worked as a postdoctoral researcher with Prof. Xiaoyuan Chen at the National Institutes of Health (NIH) for 4 years. In 2019, he joined the faculty of Tianjin University as a professor. His current research focuses on the design and development of stimuli-responsive nanomaterials for biomedical applications.



Xiaoyuan Chen received his Ph.D. in chemistry from the University of Idaho (1999). He joined the NIH in 2009 as a senior investigator and chief of the Laboratory of Molecular Imaging and Nanomedicine (LOMIN) at the National Institute of Biomedical Imaging and Bioengineering (NIBIB), NIH. He recently moved to the National University of Singapore as Nasrat Muzayyin Professor in Medicine and Technology. His current research interests include the development of a molecular imaging toolbox for the better understanding of biology, the early diagnosis of disease, the monitoring of therapy response, and the guidance of drug discovery/development.



**Scheme 1.** Pyroptosis pathway. In the canonical pathway, upon sensing DAMPs or PAMPs, caspase-1 is recruited and activated. Then caspase-1 promotes the maturation of the precursors of IL-1 $\beta$  and IL-18 and cleaves GSDMD. The N-domain of GSDMD interacts with the plasma membrane to form cell membrane pores, which leads to the release of intracellular contents, including IL-1 $\beta$  and IL-18. The non-canonical pathway is triggered by caspase-4/5/11 upon self-detection of cytosolic LPS. Activated caspase-4/5/11 successively cleaves GSDMD and induces pyroptosis. The other pathways of pyroptosis can be engaged through mechanisms such as caspase-8/GSDMD or caspase-3/GSDME. Reproduced with permission from Ref. [9d]. Copyright 2019, Springer Nature.

clitaxel,<sup>[23]</sup> and doxorubicin,<sup>[24]</sup> can trigger GSDMD/GSDME-mediated pyroptosis in a wide variety of cancer cells. However, there are some obstacles that need to be overcome during the delivery of small molecules, including rapid clearance from blood circulation, non-specific biodistribution, and systemic adverse reactions caused by high drug dosage. Nanotechnology may be able to offer a satisfying answer to the above challenges. Initially, the goal for nanotechnology was to deliver diagnostic and therapeutic agents in a more efficient and safer manner.<sup>[25]</sup> This blueprint has become more realistic in recent years, with growing numbers of nanodiagnosics and nanotherapeutics being translated into products or having been applied in clinical settings.<sup>[26]</sup> Thanks to the rapid development of biomaterials and nanotechnology, nanocarriers have shown unique advantages in the field of cancer therapy, such as reducing drug toxicity, improving drug bioavailability and specificity, increasing accumulation of anti-carcinogen in tumors via the enhanced permeability and retention (EPR) effect,<sup>[27]</sup> reducing non-specific reactions with proteins or the reticuloendothelial system (RES), and realizing active targeting to tumors through simple and appropriate modifications.<sup>[28]</sup> An emerging anticancer strategy for the activation of pyroptosis is the application of nanomedicines. In general, smart nanomedicines can deliver pyroptotic reagents into tumor cells, where pyroptotic reagents can be activated by various endogenous or exogenous

stimuli to regulate the expression of caspase proteins which mediate the process of pyroptosis. Although there are many reviews which introduce the close relationship between pyroptosis mechanism and various cancers, a summary covering recent progress in the field of nanomedicines for cancer therapy has not yet been presented.

In this Minireview, we summarize excellent studies which have taken advantage of different nanotechnologies to treat cancers based on the pyroptosis mechanism over the past years (Table 1). In addition, some inspiring contributions on the pyroptosis-based toxicological assessment of inorganic nanoparticles are also discussed in this Minireview because of their close relationship with human health. After nearly 30 years of flexuous exploration, pyroptosis mechanisms have now been clearly elucidated. Pyroptosis will certainly provide new strategies for treating cancer in the clinic.

## 2. Nanomaterials for Pyroptosis-Based Cancer Therapy

### 2.1. Liposome-Based and Polymer-Based Nanoformulations

Owing to the hypermethylation of the *DFNA5* gene, the GSDME protein expression in most tumor cells in the caspase-3 involving pyroptosis pathway is far lower than in

**Table 1:** Summary of the discussed nanomaterials and their related pyroptosis mechanisms.

| Nanomaterials                                 | Gasdermin | Pyroptosis mechanism | Immunostimulatory effect   | Cancer type             | Ref. |
|---|-----------|----------------------|--|-------------------------|------|
| DAC/LipoDDP                                   | GSDME     | Caspase-3            | IL-1 $\beta$ , HMGB1   | 4T1                     | [29] |
| ICG + DAC/PLGA + cell membrane                | GSDME     | Caspase-3            | IL-6, TNF- $\alpha$ , IFN- $\gamma$ , CD11c <sup>+</sup> , CD4 <sup>+</sup> , CD8 <sup>+</sup>   | 4T1                     | [30] |
| GOD/ROS-responsive polyion complex            | –         | Oxidative DNA damage | IL-1 $\beta$ , HMGB1   | 4T1                     | [32] |
| As <sub>2</sub> O <sub>3</sub> /mPEG-PLGA-PLL | GSDME     | Caspase-3            | –  | HCC                     | [33] |
| Iron oxide/PEG-amine/Gastrin                  | –         | Caspase-1            | Independence of IL-1 $\beta$   | INR1G9-CCK2R            | [34] |
| MIL-100(Fe) MOF/DOPC                          | Gasdermin | Caspases             | IL-1 $\beta$   | HeLa                    | [35] |
| DITOX + PE24/T22                              | –         | Caspase-11           | –  | CXCR4 <sup>+</sup> Da13 | [37] |
| NPs/GSDMA3                                    | GSDMA3    | –                    | CD3 <sup>+</sup> T, CD4 <sup>+</sup> T, CD8 <sup>+</sup> T, CD4 <sup>+</sup> FOXP3 <sup>+</sup> T <sub>reg</sub> , NK cells, M1 and M2 macrophage, IL-1 $\beta$ , IL-18, HMGB1 | 4T1                     | [38] |
| SLR20/pH-copolymer                            | GSDMD     | Caspase-1            | CD4 <sup>+</sup> , CD8 <sup>+</sup> , CD45 <sup>+</sup>  | MCF7, BT474, 4T1        | [39] |

normal cells, which possibly causes the severe side effects and unsatisfactory treatment efficacy. Zhang et al. developed a strategy in which decitabine (DAC) was combined with a chemotherapy nanodrug that was capable of triggering the pyroptosis pathway of cancer cells to amplify the immune effect of chemotherapy and eventually ablated tumors through immune therapy (Figure 1a).<sup>[29]</sup> DAC, one of the most frequently used DNA methyltransferase (DNMT) inhibitors, can inhibit methylation of the *DNMT5* gene and recover normal expression of the GSDME protein at a low dose. A tumor-targeted nanoliposome carrying cisplatin, namely LipoDDP, was used to activate the caspase-3-involving pyroptosis in cancer cells, driving tumor cell swelling and cell content leakage (Figure 1a,b). Benefiting from the advantages of liposomes, LipoDDP showed good biocompatibility, high drug loading efficiency and stability, long blood circulation time, and an enhanced EPR effect. Upon treatment with DAC + LipoDDP, the relevant genes in different cell death modes (apoptosis, necrosis, and pyroptosis) were upregulated overall, demonstrating that the pyroptosis process was accompanied by apoptosis and necrosis, which is usually called “secondary necrosis” (Figure 1c). Interestingly, the combined treatment greatly boosted DC maturation (CD11c<sup>+</sup>CD80<sup>+</sup>CD86<sup>+</sup>) in the lymph nodes and induced native CD8<sup>+</sup>T cells to transform into the central memory CD8<sup>+</sup>T cells in the spleen (Figure 1d,e), suggesting that the combination of DAC and LipoDDP activates the immunological response of living systems. The results of *in vivo* studies demonstrated that LipoDDP treatment after DAC pretreatment not only achieved excellent tumor suppression, but also efficiently suppressed tumor metastasis. Based on the antitumor and antimetastasis activities, this combined therapy increases the systemic immune response of chemotherapy and offers a new hope for tumor immunotherapy.

Owing to the existence of immune suppressor cells in the tumor microenvironment, e.g. M2 macrophages, myeloid-derived suppressor cells, and Tregulatory cells, the systemic immune response of most tumors is downregulated or inhibited. Although several strategies, including immune checkpoint blockade therapy, have been proposed to increase the immune activity of tumors, activating their immune response is still a crucial challenge. Being able to release proinflammatory intracellular contents, pyroptosis is an excellent choice for cancer immunotherapy. Chemotherapeutic drugs are usually employed to induce pyroptosis. However, innate drug resistance and severe toxicity hinder their development in biomedical applications. Qu et al. designed a biomimetic nanoparticle (BNP) which combined photodynamic therapy with chemotherapy in order to regulate cell pyroptosis for further cancer immunotherapy (Figure 2a).<sup>[30]</sup> BNP contained a poly(lactic-co-glycolic acid) (PLGA) polymeric core and a cell membrane shell. The chemotherapeutic drug DAC and indocyanine green (ICG) were co-loaded in the hydrophobic nuclei of BNP. The cell membrane shell endowed BNP with low immunogenicity and tumor targeting capability, and ICG was able to transform low-dose photons into local hyperthermia at the tumor site. Thanks to the tumor targeting capability of the cell membrane with low immunogenicity, BNP effectively accumulated in the tumor and ICG inside BNP pierced the tumor cell membrane to induce a sudden increase in cytoplasm Ca<sup>2+</sup> concentration supported by low-dose NIR irradiation. Then cytochrome *c* release was promoted and caspase-3 was activated. Meanwhile, upregulated GSDME expression by DAC enhanced the caspase-3-catalyzed GSDME cleavage, which eventually caused pyroptosis. Owing to the demethylation feature of DAC, GSDME expression was greatly increased after incubation with BNP. However, the expression of GSDME was again dramatically

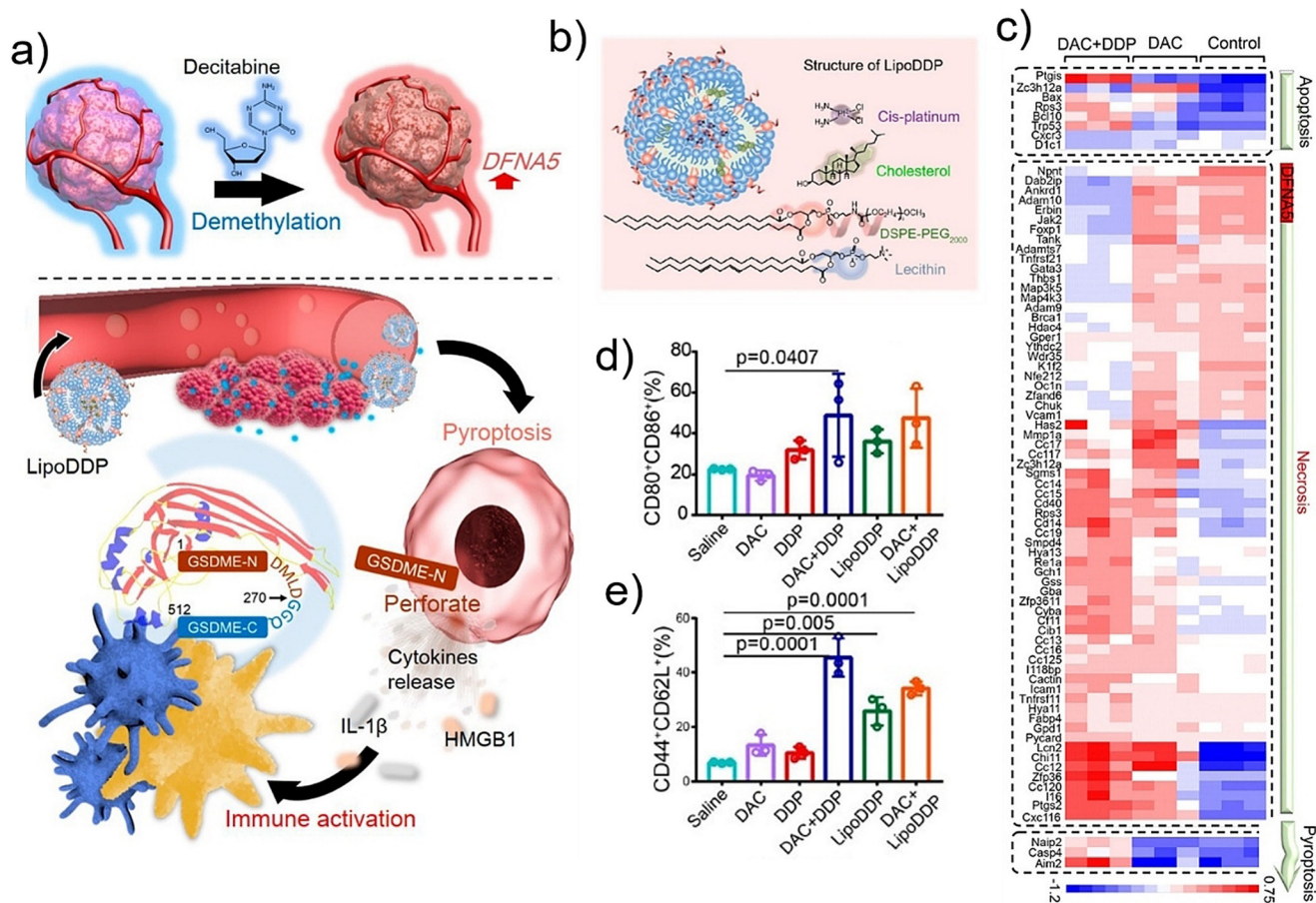


**Figure 1.** a) Demethylation process of DAC and the immune activation process induced by LipoDDP on the basis of the pyroptosis pathway. b) Composition of LipoDDP. c) Heat maps of specific genes related to pyroptosis, necrosis, and apoptosis. d) Quantification of CD80<sup>+</sup>CD86<sup>+</sup> cells gating on CD11c<sup>+</sup> cells within a tumor-draining lymph node (TDLN). e) Quantification of CD44<sup>+</sup>CD62L<sup>+</sup> cells gating on CD8<sup>+</sup> cells within the spleen. Reproduced with permission from Ref. [29]. Copyright 2019, American Chemical Society.

decreased (Figure 2b) while the GSDME N-terminal concentration (Figure 2c) and caspase-3 cleavage were obviously increased after photoactivation, which indicated that the pyroptosis pathway was activated by the photothermal treatment. Interleukin 6 (IL-6) and tumor necrosis factor  $\alpha$  (TNF- $\alpha$ ) secreted by BMDCs and the CD86 and CD11c expressions on the BMDC surface were all increased, which indicates that photoactivated pyroptosis provides a promising strategy for immune system activation and cancer immunotherapy. In vivo, the growth of primary tumor and distant tumor was efficiently suppressed. Moreover, no obvious tissue injury or weight loss was observed, suggesting BNP was highly biocompatible. After BNP + photoactivation, high percentages of CD4<sup>+</sup>T cells and CD8<sup>+</sup>T cells in spleens and distant tumors were detected, and isolated splenocytes induced significant cell death and secreted a high level of interferon- $\gamma$  (IFN- $\gamma$ ) (Figure 2d), suggesting that this strategy was able to activate systemic T cells for the immunotherapy of solid tumors. Considering the high potential in antitumor and antimetastasis activity as well as systemic T-cell activation, this pyroptosis-associated BNP provides a novel strategy for cancer immunotherapy with good biocompatibility and broad clinical applicability.

Polymer vesicles provide strategies for the construction of biologically smart nanodevices with specific and precise functions. Some excellent therapeutic nanoreactors have been proposed to achieve novel orchestrated oxidation/chemotherapy/gas therapy of cancer via specific activation at tumor sites with the aid of synergistic effects.<sup>[31]</sup> However, the engineering of nanoreactors with a permeability controllable without destroying the structural integrity and functionality still remains a challenge. Kataoka et al. reported an ingenious strategy to construct a ROS-responsive nanoreactor on the basis of polyion complex vesicles (PICsomes) by introducing thioketal linkers into the covalent crosslinking membrane network (Figure 3a).<sup>[32]</sup> Owing to the existence of thioketal linkers, PICsomes showed H<sub>2</sub>O<sub>2</sub>-responsive swelling without structural rupture, realizing a size-selective release. Glucose, the target zymolyte of glucose oxidase (GOD), can be degraded into H<sub>2</sub>O<sub>2</sub> with the help of O<sub>2</sub>. To meet the needs of intensive metabolic activity, glucose concentrations at tumor sites are usually high. When GOD-loaded PICsomes reached the tumor site, high concentrations of glucose slowly crossed the membrane of PICsomes and were catalytically converted into H<sub>2</sub>O<sub>2</sub>. At the same time, the cascade reactions increased the membrane permeability, which further accel-

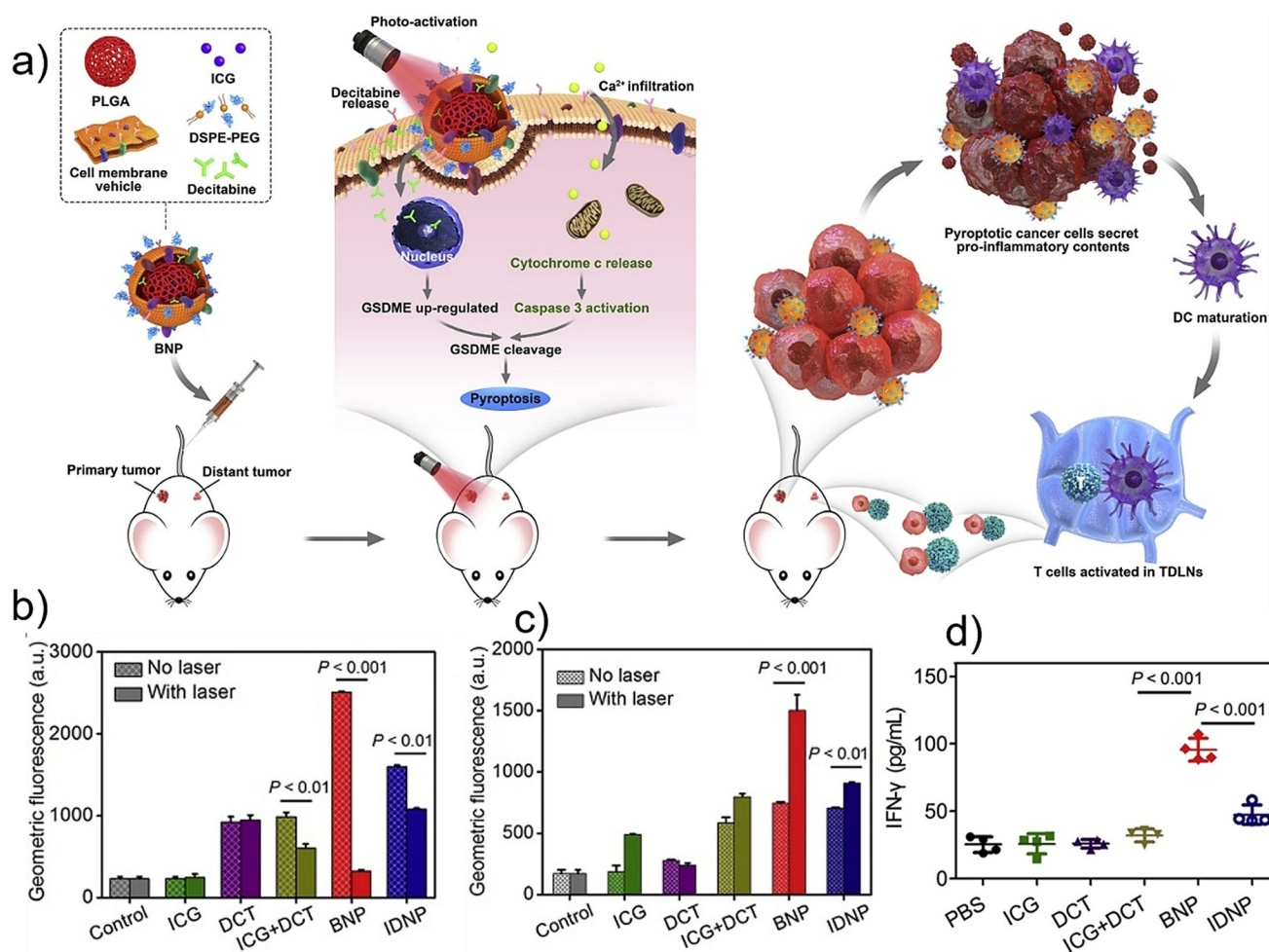


**Figure 2.** a) The mechanism of tumor therapy mediated by photoactivated pyroptosis. b) Intracellular GSDME concentration and c) GSDME N-terminal concentration analysis after different treatments. d) IFN- $\gamma$  levels secreted by CD4<sup>+</sup> and CD8<sup>+</sup> splenocytes after co-incubation with cancer cells. Reproduced with permission from Ref. [30]. Copyright 2020, Elsevier.

erated this process, endowing the nanoreactors with a self-boosting ability to increase oxidative stress and trigger glucose starvation at the tumor site, which eventually resulted in pyroptotic death of tumor cells. Upon exposure to H<sub>2</sub>O<sub>2</sub>, the vesicle size increased steadily and reached a peak at 130 nm, regardless of H<sub>2</sub>O<sub>2</sub> concentration, which suggests that H<sub>2</sub>O<sub>2</sub> stimulation can relax the PICsomes but not destroy the integrity of the structure. Because of the size-dependent cargo release and vesicle swelling without collapse, ROS-responsive PICsomes carrying GOD were capable of self-boosting catalytic glucose oxidation and could be used for cancer treatment through oxidative stress induction and glucose starvation strategies. Although the IC<sub>50</sub> value of PICsomes was higher than that of GOD, the GOD-carrying PICsomes guaranteed a long lasting cytotoxicity of GOD (Figure 3b). Severe oxidative DNA damage was induced by nanoreactors (Figure 3c) and this was the main cause of cytotoxicity. The morphology of cells changed with large bubbles (Figure 3d) and both calreticulin expression and HMGB1 concentration were increased (Figure 3e,f), which confirmed that pyroptotic death occurred in the tumor cells. Therefore, these GOD-loaded PICsomes can act as therapeutic nanoreactors with the

ability of self-reinforcement, acceleration of ROS production, and persistent cytotoxicity in order to induce immunostimulatory pyroptotic tumor cell death.

## 2.2. Metal-Oxide-Based Nanoparticles

As<sub>2</sub>O<sub>3</sub> can promote the differentiation of surviving tumor cells and reduce malignancy and cancer cell metastasis during chemotherapy. In order to retain the therapeutic As<sub>2</sub>O<sub>3</sub> concentration within solid tumor tissues during treatment to avoid its systemic toxicity, Duan et al. constructed a nano-drug delivery system in which the triblock copolymer mPEG-PLGA-PLL was employed to load As<sub>2</sub>O<sub>3</sub> (As<sub>2</sub>O<sub>3</sub>-NPs). Thanks to the mPEG-PLGA-PLL coating, As<sub>2</sub>O<sub>3</sub>-NPs possessed several excellent features, such as high stability in physiological environments, long circulation time and high tumor accumulation. After the internalization of As<sub>2</sub>O<sub>3</sub>-NPs by tumor cells, As<sub>2</sub>O<sub>3</sub> was released into the cytoplasm and caspase-3 was activated. Thereafter, GSDME cleavage was triggered by the activated caspase-3 and N-domains of GSDME were released, which inserted into the cell mem-

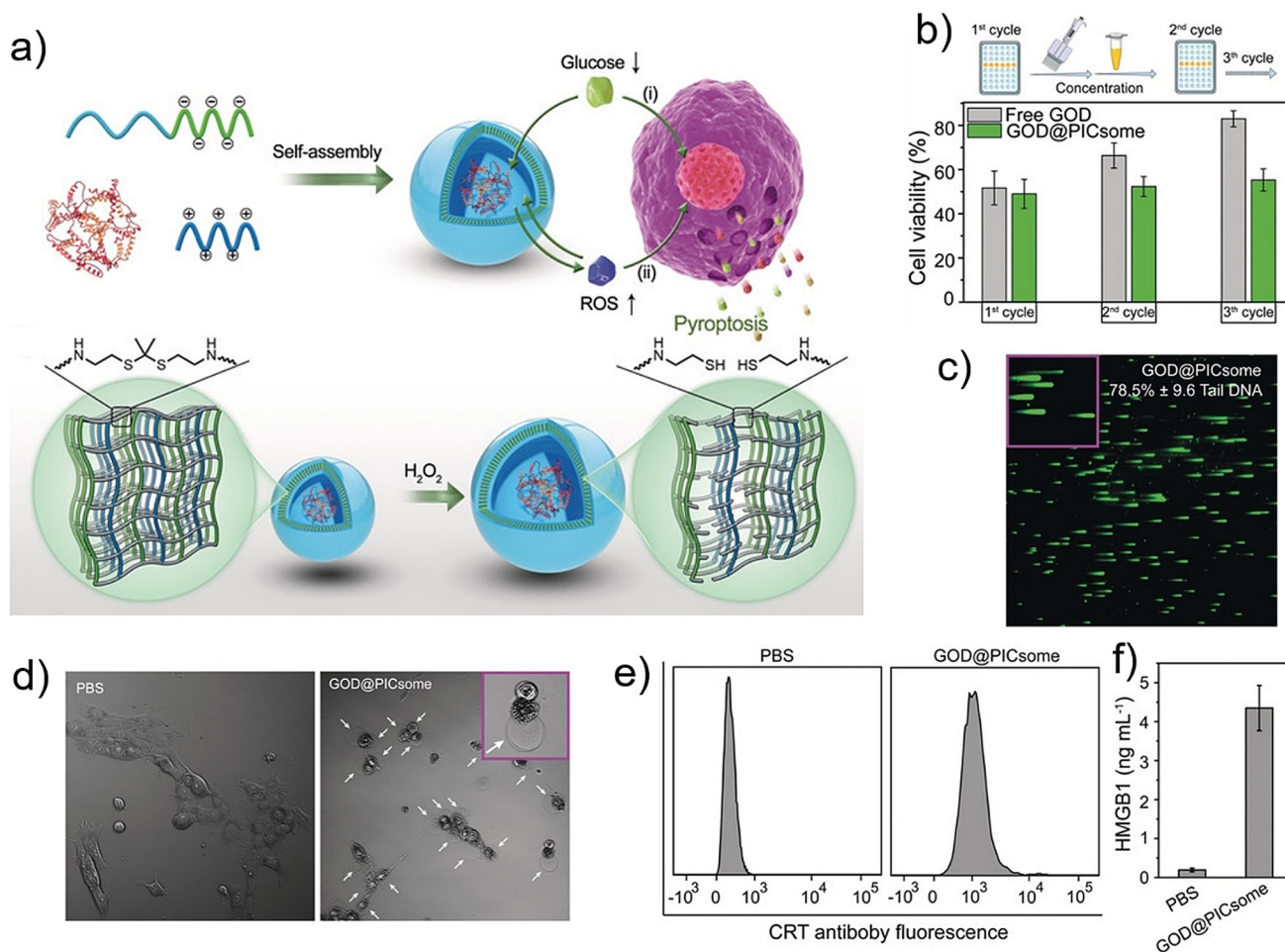


**Figure 3.** a) Mechanistic diagram of the cytotoxic function of a ROS-responsive GOD-loaded nanoreactor with self-boosting catalytic glucose oxidation capability. b) Cytotoxicity of recycled GOD and GOD@PICsomes from old culture medium at their  $IC_{50}$  concentration. c) The Comet Assay of 4T1 cells treated with GOD@PICsomes. d) Bright-field images of 4T1 cells treated with GOD@PICsomes. e) The calreticulin level and f) HMGB1 level of 4T1 cells treated with GOD@PICsomes. Reproduced with permission from Ref. [32]. Copyright 2020, Wiley VCH.

brane to form membrane pores, eventually leading to pyroptosis-based cell death. The therapeutic efficacy and mechanism of  $As_2O_3$ -NPs in the treatment of hepatocellular carcinoma (HCC) is shown in Figure 4a, I.<sup>[33]</sup> Compared with free  $As_2O_3$ ,  $As_2O_3$ -NPs displayed decreased Dnmt1, Dnmt3a, and Dnmt3b expressions and an enhanced GSDME-N level in Huh7 and HepG2 cells. In vivo studies showed that  $As_2O_3$ -NPs not only enhanced antitumor activities through GSDME cleavage (Figure 4a, II), but also downregulated DNA methyltransferase expression (Figure 4a, III). More intriguingly, a H&E stain assay verified that  $As_2O_3$ -NPs exhibited no obvious systemic toxicity. These data show the promising performance of  $As_2O_3$  in hepatoma cells, which can be explored for further therapies of hepatocellular carcinoma on the basis of the pyroptosis pathway.

The application of drugs to induce lysosomal cell death has been an effective therapeutic strategy to kill drug-resistant tumor cells. Magnetic intra-lysosomal hyperthermia (MILH) triggered by magnetic nanoparticles (MNPs) has emerged as a promising therapeutic option. Gigoux et al. designed a nanoplatform in which magnetic iron oxide nanoparticles were wrapped by PEG-amine and further

functionalized by gastrin and NHS-DY647-PEG1 (Gastrin-MNPs).<sup>[34]</sup> The PEG coating prolonged blood circulation and enhanced biocompatibility of the Gastrin-MNPs. In order to accurately target CCK2R overexpressed on the surface of tumor cells, gastrin, a specific ligand of CCK2R, was used as the targeting peptide of MNPs. The Gastrin-MNPs were selectively endocytosed by INR1G9-CCK2R cells guided by peptides and were then transported into lysosomes where they accumulated. When exposed to an alternating magnetic field (AMF), Fenton reactions were activated and ROS were generated, which caused the collapse of the lysosomal membrane and leakage of lysosomal enzyme (cathepsin-B), finally resulting in caspase-1-mediated pyroptosis. First, it was demonstrated that MILH initially generated ROS with the aid of the Fenton reaction within cytolysosomes where Gastrin-MNPs had accumulated (Figure 4b, I). Thereafter, lysosomal membrane collapse and cathepsin-B leak into the cytosol were both verified to be related with MILH. Further studies demonstrated that cell death triggered by MILH did not belong to the caspase-3-dependent apoptotic pathway but relied on cathepsin-B activity which activated the caspase-1-dependent pyroptosis pathway (Figure 4b, II). Collectively,

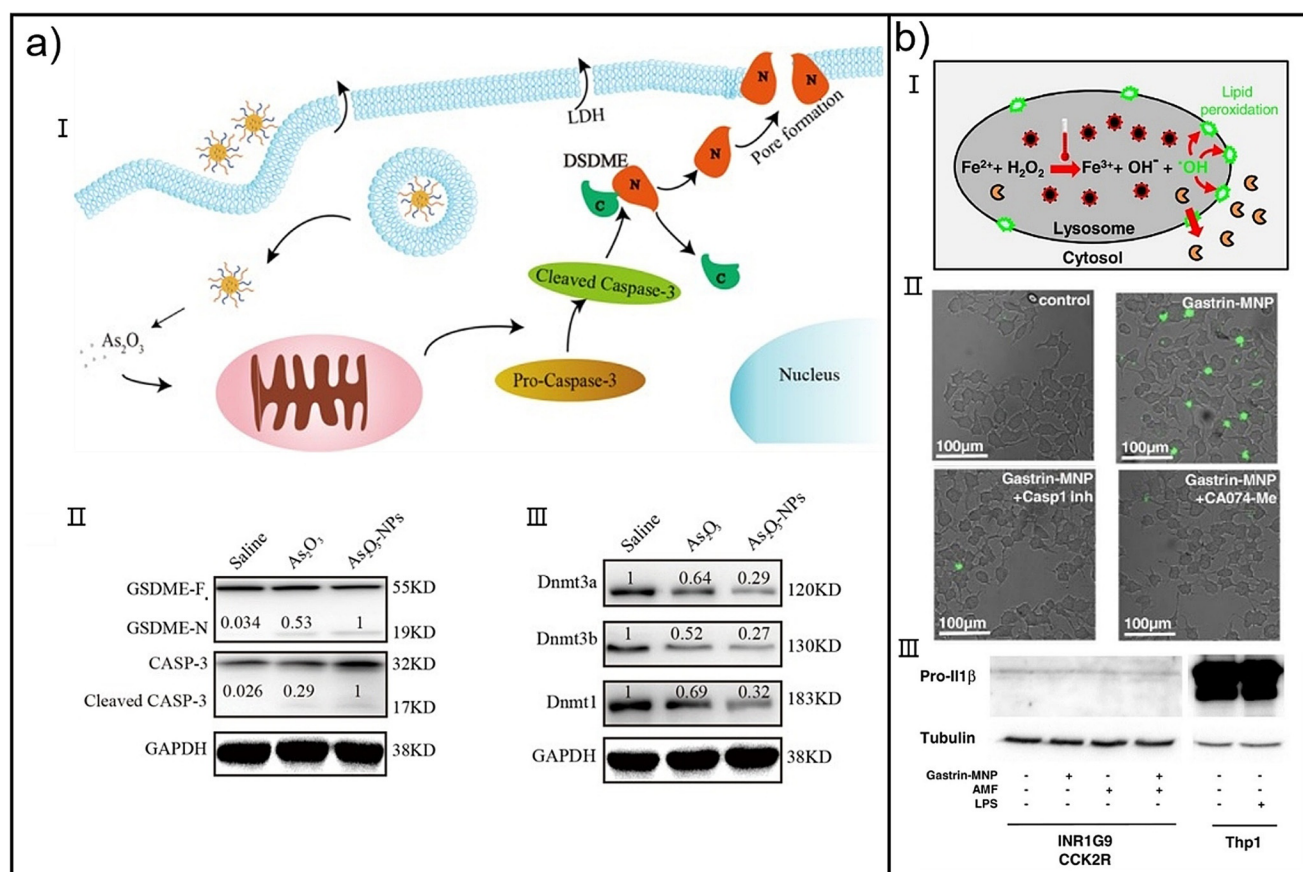


**Figure 4.** a) As<sub>2</sub>O<sub>3</sub>-NPs for the induction of apoptosis. I) The mechanism of pyroptosis induced by As<sub>2</sub>O<sub>3</sub>-NPs in HCC. II) The expression of GSDME-F, GSDME-N, caspase-3, and cleaved caspase-3 in a Huh7 tumor. III) The expression levels of Dnmt3a, Dnmt3b, and Dnmt1 in a Huh7 tumor. b) Gastrin-MNPs for the induction of pyroptosis. I) Hypothesis of an initiating event triggered by MILH in the lysosome. II) Confocal images of cells labeled with FAM-FLICA-Casp1. III) Pro-IL-1β expression after different treatments. Reproduced with permission from Ref. [33]. Copyright 2019, Springer Nature. Reproduced with permission from Ref. [34]. Copyright 2018, Elsevier.

these data demonstrate that Gastrin-MNPs induce the pyroptosis pathway of INR1G9-CCK2R cells. It is noteworthy that caspase-1-dependent pyroptosis induced by MILH was not able to increase the expression of pro-IL-1β (Figure 4b, III). Considering the inherently low level of IL-1β in INR1G9-CCK2R cells, proinflammatory effects may be induced by MILH in other tumor cells with a high level of pro-IL-1β expression. Similar to the CCK2R-overexpressing INR1G9-CCK2R cells, the cell death of three other tumor cell lines (AGS-CCK2R, HEK-CCK2R, and AR4-2J cells) with low CCK2R expression was also induced by MILH with the same caspase-1-dependent pyroptosis pathway. This study clearly reveals the mechanism of the MILH-triggered cancer cell death. Fenton reaction, cathepsin-B, and caspase-1 form the basis of this MILH strategy for the eradication of tumor cells and can be further developed into novel therapeutic strategies to combat malignancy.

Ion homeostasis is important for cell proliferation, and inducing ion imbalance is usually applied to trigger instinct form of PCD. Nevertheless, research into the influence of specific ions on cells in a well-controlled manner has been hindered by the cells' meticulous adjustment of ion transportation. Hybrid MOF nanoparticles provide an option to realize direct and controlled ion delivery into cells. Engelke

et al. designed and synthesized a lipid-coated MIL-100(Fe) MOF nanomaterial using Fe<sup>3+</sup> and trimesic acid as building blocks (Lip-MOFs), which is capable of introducing the majority of its Fe<sup>3+</sup> ions into cells. To inhibit cellular identification of the surface ions of MOF nanoparticles and to facilitate cellular endocytosis, nanoparticles were packaged with 1,2-dioleoyl-*sn*-glycero-3-phosphocholine (DOPC) (Figure 5a, I).<sup>[35]</sup> Lip-MOFs benefit from the advantages of liposome-based nanotechnology and exhibited good biocompatibility as well as a significant EPR effect. After cellular uptake by clathrin-mediated endocytosis, Lip-MOFs were transported into the lysosomes where they were degraded into Fe<sup>3+</sup> ions and trimesic acids by a reduction process involving cysteine. It is noteworthy that the intracellular degradation of Lip-MOFs and iron release could be controlled by the acidic extracellular environment. A large number of Fe<sup>3+</sup> ions triggered lysosomal rupture and induced subsequent pyroptosis, which was mediated by caspase activation, GSDM cleavage and IL-1β release. For better visualization, calcein was loaded prior to DOPC coating so that the dye was first quenched by the MOFs and then fluorescence was turned on upon disintegration of the MOFs. After an incubation time of 40 h, Lip-MOFs collapsed and the fluorescence was turned on in the acidic lysosome, which

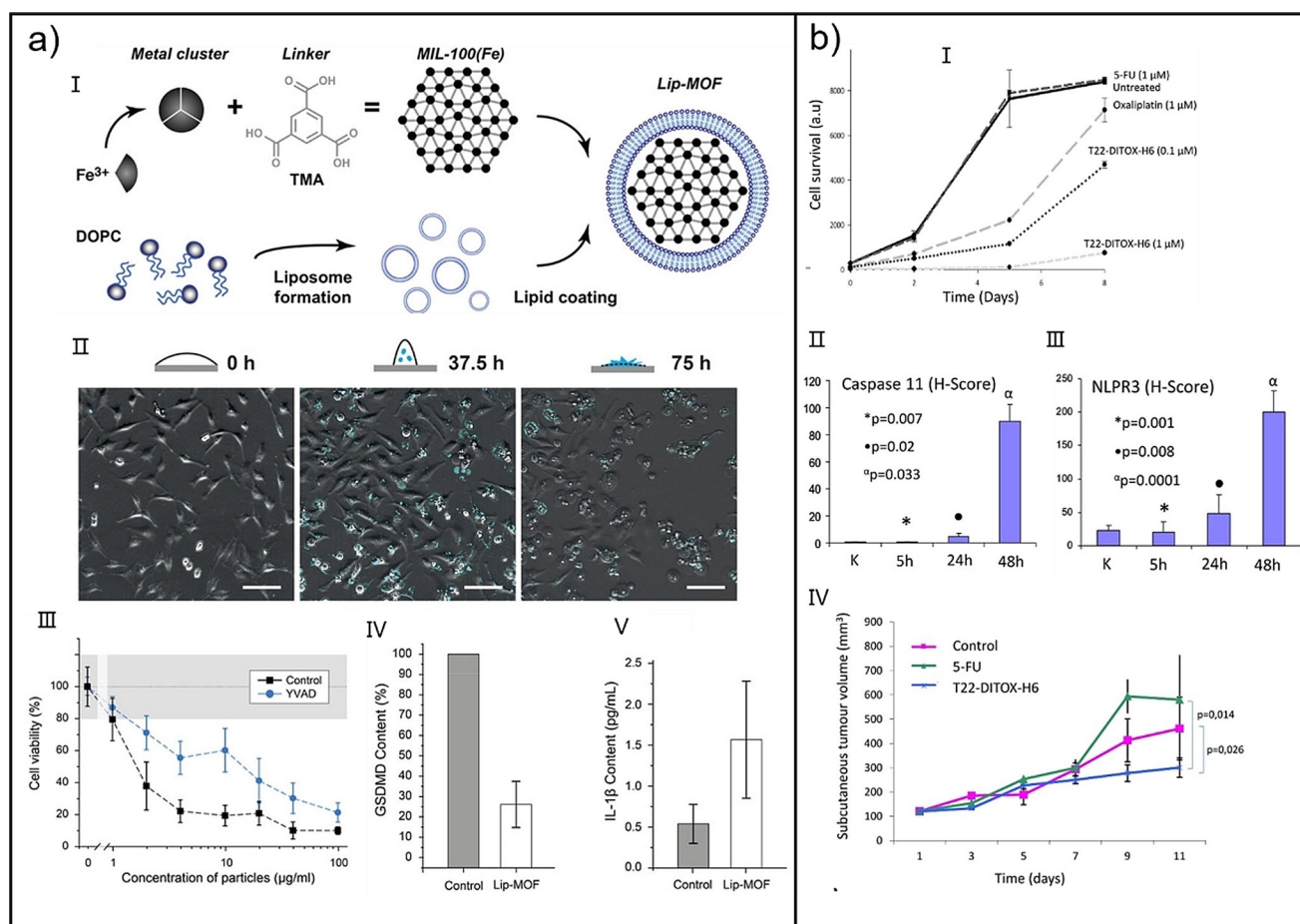


**Figure 5.** a) Lip-MOFs for the induction of pyroptosis. I) Synthetic route to Lip-MOF nanoparticles. II) Time-lapse images of HeLa cells treated with Lip-MOFs. III) MTT assay of HeLa cells after different treatments. IV) GSDMD content of HeLa cells after different treatments. V) IL-1 $\beta$  content of HeLa cells after different treatments. b) T22-DITOX-H6 for pyroptosis-mediated cancer therapy. I) Cell survival after different treatments. II, III) Caspase-11 and NLRP3 expression in Da13 tumors after different treatments. IV) Tumor volume curve after different treatments. Reproduced with permission from Ref. [35]. Copyright 2020, Wiley VCH. Reproduced with permission from Ref. [37]. Copyright 2020, Elsevier.

indicates that the Lip-MOFs were phagocytosed and reached the lysosome. Within seconds, the fluorescence extended all over the cells, suggesting disintegration of the lysosomes (Figure 5a, II). Interestingly, the iron release triggered by Lip-MOF collapse in the lysosome was mediated by cysteine-based reduction, which was reinforced in the slightly acidic extracellular environment. Pre-treatment of  $\alpha$ -YVAD-FMK (an inhibitor for pyroptosis-inducing caspases) enhanced the cell viability (Figure 5a, III), reduced the full length GSDMD (Figure 5a, IV), and increased the IL-1 $\beta$  release (Figure 5a, V), collectively demonstrating that pyroptosis dominated the cell death pathway. Different from A549 and MCF-10A cells, A431, MCF7, and macrophage cells showed clear pyroptosis morphology after incubation with Lip-MOFs. Because macrophages play an important role in the tumor immune system, Lip-MOFs may elicit an immune response on condition that most of the Lip-MOFs are endocytosed by macrophages. Hence, Lip-MOFs and other similar nanocomposites may be used to attack cancer cells in the acidic microenvironment for immunotherapy based on the pyroptosis pathway.

### 2.3. Protein-Based Nanoparticles

Cancer stem cells (CSCs) have been identified as the root of carcinoma because of their superior self-renewal ability and clonogenic features. Because of drug resistance, existing treatments cannot effectively eliminate colorectal CSCs. According to the studies, CXCR4 overexpression is closely associated with unfavorable prognosis and drug resistance in colorectal cancer (CRC).<sup>[36]</sup> To overcome the above difficult problems, Serna et al. constructed a toxin-based nanocarrier, in which pseudomonas exotoxin (PE24) and diphtheria toxin (DITOX) acted as the therapeutic building blocks and were fused with the CXCR4 ligand T22 (T22-DITOX-H6). T22-DITOX-H6 selectively bound to CXCR4<sup>+</sup> CRC-CSC via T22, thereby improving phagocytosis efficiency and reducing systemic toxicity. The released PE24 and DITOX in the cytosol suppressed the eukaryotic elongation factor 2 (eEF-2), which hindered protein synthesis and eventually resulted in pyroptosis mediated by caspase-11 and NLRP3. Owing to the synergetic action of CXCR4<sup>+</sup> targeting and the efficient killing effect of toxins, T22-DITOX-H6 greatly inhibited cell survival, which indicates that the use of targeting toxin-based

nanocarriers is a viable method for colorectal CRC therapy (Figure 5b, I).<sup>[37]</sup> In addition, the increased expression of NLPR3 and caspase-11 in CXCR4<sup>+</sup> CRC-CSC (Da13) tumors indicated that T22-DITOX-H6 was able to induce a pyroptosis but not an apoptosis process in colorectal CSCs (Figure 5b, II and III), thus showing great potential to overcome tumor drug resistance. According to *in vivo* studies the T22-DITOX-H6 group showed significant tumor inhibition (Figure 5b, IV) and low systemic toxicity compared with 5-fluorouracil (5-Fu). These results demonstrate that CXCR4-targeted T22-DITOX-H6 nanoparticles can effectively erase apoptotic-resistant CXCR4<sup>+</sup> CRC CSCs by inducing pyroptosis. Hence, the application of multi-pathway therapeutic agents may be a powerful and smart strategy in CXCR4<sup>+</sup> CRC-CSC treatment.

Bioorthogonal chemistry which can be applied in living systems has been pursued to explore biological processes such as immunity and cell death. Pyroptosis is a proinflammatory cell death mediated by the gasdermin family. However, the relationship between this proinflammatory cell death and antitumor immunity is unknown. A bioorthogonal chemical system that can explore the mechanism of antitumor immunity of pyroptosis is therefore needed. For this purpose, Shao et al. established a nanobioorthogonal chemical system (NP-GSDMA3), in which gasdermin A3 (GSDMA3) was linked to

nanoparticles through the triethylsilyl (TES) ether linker in order to achieve a controlled and efficient GSDMA3 release. Benefiting from its nanoscale size, NP-GSDMA3 showed high accumulation in tumor sites through the EPR effect. The tumor-imaging probe phenylalanine trifluoroborate (Phe-BF<sub>3</sub>) could selectively enter into cells and effectively cleave the silyl ether bond of NP-GSDMA3 to release GSDMA3 protein, which was able to form membrane pores followed by pyroptosis. Because of the release of inflammatory cytokines, pyroptosis activated the antitumor immune response of living systems, which cooperated with checkpoint blockade to enhance the efficiency of cancer immunotherapy (Figure 6a, I).<sup>[38]</sup> When HeLa, EMT6, 4T1, and BMDM cells were cultured with NP-GSDMA3 and Phe-BF<sub>3</sub>, membrane enrichment of N domains of gasdermin and a pyroptotic morphology of the cells were clearly observed (Figure 6a, II). Intratumoral and intravenous injection resulted in similar regression of 4T1 tumors, suggesting the tumor inhibitory effect was a result of GSDMA3 activation at the tumor location. NP-GSDMA3 and Phe-BF<sub>3</sub> induced only 20% propidium iodide-positive pyroptotic cells in the tumor but could erase the entire tumor tissue, implying that the immune system was involved in this process. It was found that the population of CD4<sup>+</sup>T, CD8<sup>+</sup>T, and natural killer cells increased, but not for neutrophil, monocyte, and myeloid-

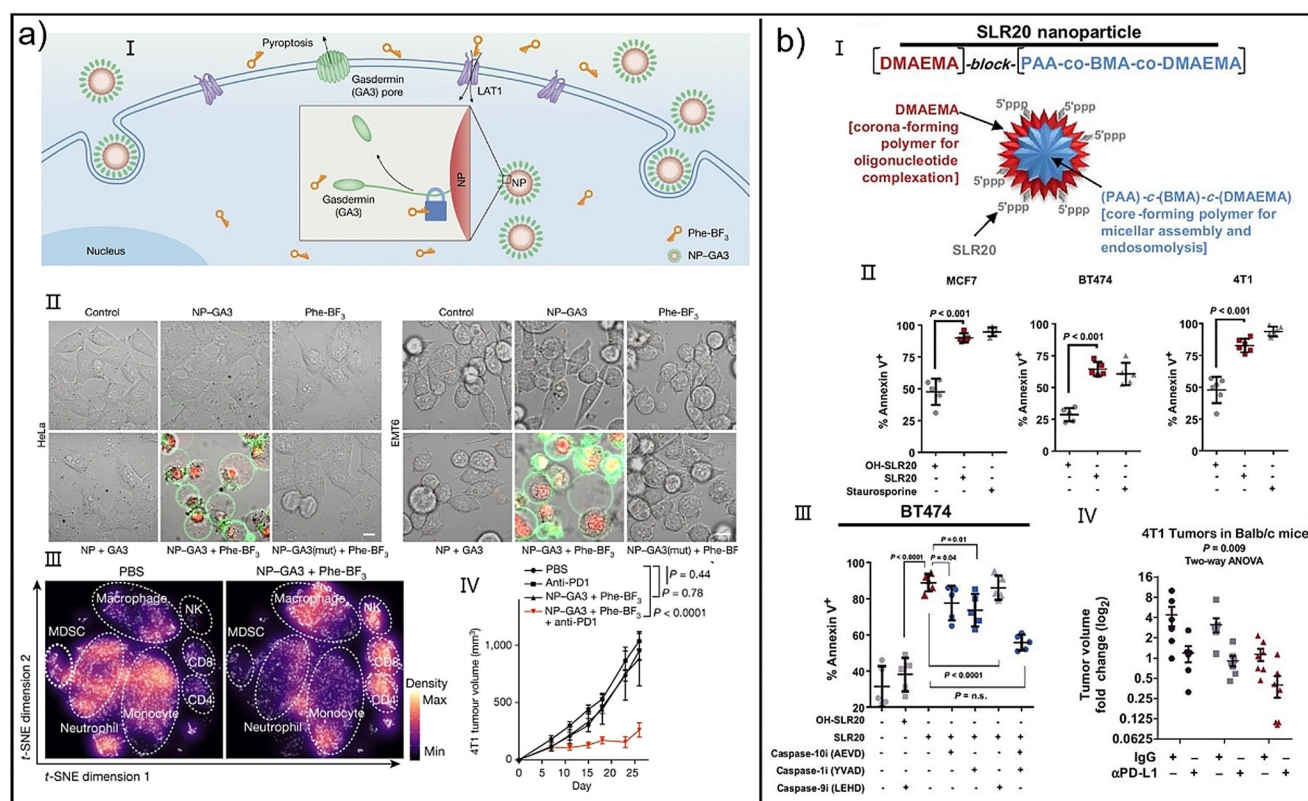


**Figure 6.** a) NP-GSDMA3 for pyroptosis-mediated cancer therapy. I) Mechanistic diagram of the experimental design and the composition of NP-GSDMA3. II) Confocal images of HeLa and EMT6 cells after different treatments. III) Single-cell RNA sequencing of CD45<sup>+</sup> immune cells isolated from 4T1 tumors after different treatments. IV) Tumor growth curve after different treatments. b) SLR20 nanoparticles for pyroptosis-mediated cancer therapy. I) Schematic representation of SLR20 nanoparticle formulation. II) Percentage of Annexin V<sup>+</sup> positive cells after different treatments. III) Percentage of Annexin V<sup>+</sup> positive cells treated with different caspase-specific inhibitors. IV) Tumor volume analysis after different treatments. Reproduced with permission from Ref. [38]. Copyright 2020, Nature. Reproduced with permission from Ref. [39]. Copyright 2020, American Association for Cancer Research.

derived suppressor cells (Figure 6a, III), which confirms the potent tumor immunosuppressive effect of NP-GSDMA3 and Phe-BF<sub>3</sub>. Moreover, injection of NP-GSDMA3 + Phe-BF<sub>3</sub> alone could not inhibit 4T1 tumor growth. However, if the above treatment was continued with an anti-PD1 therapy, tumor growth was obviously inhibited (Figure 6a, IV). This shows that inflammation induced by pyroptosis within the tumor microenvironment is able to cooperate with immune checkpoint blockade for antitumor immunotherapy. In brief, this bioorthogonal system based on Phe-BF<sub>3</sub> desilylation is a smart tool for *in vivo* biological applications. Furthermore, the application of the above system to the activation of gasdermin shows an anticancer immune response of pyroptosis, hence gasdermin agonists may be used to increase the efficiency of cancer immunotherapies.

#### 2.4. Oligonucleotide-Based Nanoparticles

Cancer immunotherapies that can induce acquired immunity have recently received more attention although they have not yet been very successful in breast carcinoma, which are poorly immunogenic and contain low levels of tumor-infiltrating lymphocytes. Innate immunity of living systems plays an important role in tumor immunotherapy; this includes the induction of immunogenic tumor cell death, type I IFNs, and the expression of lymphocyte-recruiting chemokines. New strategies capable of activating innate immunity of breast cancer cells are attracting increasing interest. After activation, retinoic-acid-inducible gene I (RIG-I) cooperates with mitochondrial antiviral signaling (MAVS) to initiate signal paths which generate proinflammatory molecules. The use of RIG-I mimetics is therefore an appealing therapeutic approach in cancer immunotherapies. For this purpose, Cook et al. reused a previously reported smart RIG-I agonist engineered from a double-stranded, triphosphorylated stem-loop RNA decorated with a 50 triphosphate sequence (SLR20).<sup>[39]</sup> The stem-loop structure enhanced the structural stability of SLR20, which guaranteed that it was active *in vivo*. For *in vivo* application, a pH-responsive amphiphilic diblock copolymer was applied to construct a SLR20-based nanoscale delivery system (SLR20 NPs) (Figure 6b, I). Owing to the nanoscale size and pH-responsiveness, SLR20 NPs had some unique features which were favorable for tumor internalization. Upon activation of RIG-I by SLR20 NPs in breast tumors, cancer cell death was induced by the combination of pyroptosis and intrinsic apoptosis. Owing to the proinflammatory function of pyroptosis, an anticancer immunological effect was activated in the 4T1 tumor. As a consequence, tumor growth and metastasis were effectively inhibited by the treatment of SLR20 NPs +  $\alpha$ PD-L1. *In vivo* studies revealed that SLR20 NPs not only upregulated RIG-I expression, but also increased STAT1 phosphorylation in 4T1 tumors, demonstrating that RIG-I signaling could be induced by SLR20 NPs in breast tumors. By means of Ki67, TUNEL, and Annexin V<sup>+</sup> staining (Figure 6b, II), it was found that SLR20 could activate the RIG-I signaling pathway in 4T1 cells and induce tumor cell death. Interestingly, the combined action of

caspase-1 and caspase-10 inhibitors in BT474 cells reduced more Annexin V<sup>+</sup> stained cells than either of them alone; this suggests that RIG-I signaling may utilize both apoptosis and proinflammatory pyroptosis pathways to significantly induce PCD (Figure 6b, III). A H&E stain and tumor inhibition experiment verified that SLR20 enhanced the immunogenicity of the tumor microenvironment (Figure 6b, IV). Additionally, MCF7 cells cultured with SLR20 showed an increase in protein expression, which was assigned to several IFN  $\beta$ -inducible chemokines that can recruit T lymphocytes, suggesting SLR20 behaved as a cytokine and chemokine modulator. These findings imply that RIG-I activation induced by SLR20 NP agonists activates the innate immunity of breast carcinoma cells and enhances the immunogenicity of breast tumors. Hence, it may be a promising strategy for the treatment of breast cancers, even for those with poor immunogenicity.

### 3. Potential Toxicity of Nanoparticles Mediated by Pyroptosis

In the past decades, a growing number of nanoparticles and nanomaterials have had an enormous impact on our daily life. For instance, metal oxide (MO<sub>x</sub>) nanoparticles engineered with versatile functions have been used for the production of consumer goods like cosmetics, dietary supplements, fuel additives, clothing, and personal care products. Furthermore, rare-earth oxides (REOs) like gadolinium contrast agents, as well as other nanoparticles like silicon dioxide (SiO<sub>2</sub>) or silver nanoparticles (AgNPs), are widely used for diagnostic and therapeutic applications such as magnetic resonance imaging (MRI) and targeted drug delivery. However, the frequent and heavy use of these nanomaterials confronts the scientific community with a serious question: is it safe to be in frequent contact with these nanomaterials and is there any risk of occupational diseases for workers involved in the industrial production of nanoparticles? For this purpose, a toxicological assessment is necessary to investigate the potential toxicity of nanoparticles. This can provide appropriate methods to increase the biosafety of nanoparticles.

#### 3.1. Mesoporous Silica Nanoparticles

There is significant concern regarding the widespread biological application of mesoporous silica nanoparticles (MSNs) because of their possible toxicological hazards. According to *in vivo* studies MSNs could cause morphological and functional damage to the liver. However, the exact mechanism of toxicological effects induced by MSNs is poorly understood. It is necessary to carefully investigate the hepatotoxicity and corresponding pathogenesis of MSNs. Ju et al. filled this gap and revealed a clear mechanistic pathway for liver injury induced by MSNs (Figure 7a, I).<sup>[40]</sup> After treatment with MSNs, stained hepatic tissue displayed obvious cell pyroptosis in hepatocytes (Figure 7a, II); this demonstrates that MSNs activate NLRP3 inflammasomes

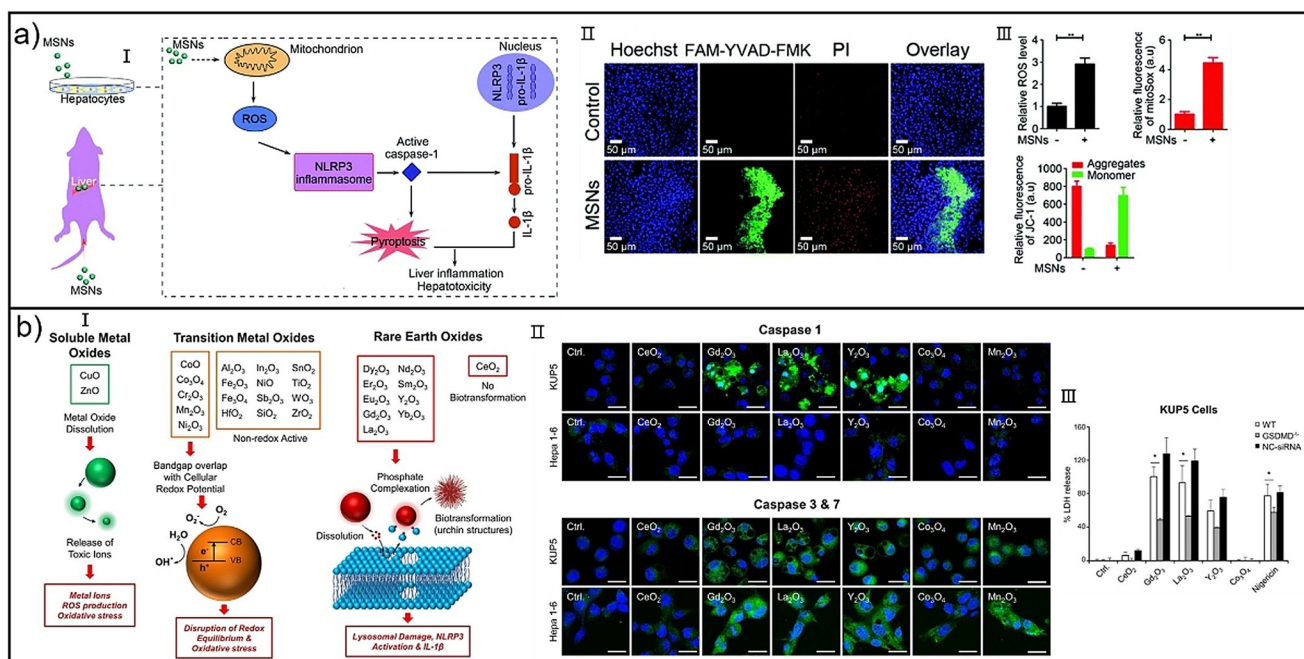


**Figure 7.** a) Evaluation of MSN hepatotoxicity. I) Mechanistic diagram of MSN-induced hepatotoxicity. II) Confocal images of liver tissues co-stained with FAM-YVAD-FMK and PI. III) ROS level and analysis of mitochondrial membrane potential after MSN treatment. b) Evaluation of REO and TMO nanoparticles on KUP5 and Hepa 1–6 cells. I) Mechanistic diagram of TMO and REO toxicity. II) Confocal images of the exposure of REO and TMO nanoparticles to KUP5 and Hepa 1–6 cells. III) LDH release behavior of KUP5 cells after different treatments. Reproduced with permission from Ref. [40]. Copyright 2018, The Royal Society of Chemistry. Reproduced with permission from Ref. [41]. Copyright 2018, American Chemical Society.

and trigger the pyroptosis pathway inside the liver. Inconsistent with WT mice, several key indexes of NLRP3<sup>-/-</sup> mice, such as NLRP3 inflammasome activation, cleaved caspase-1, IL-1 $\beta$ , serum alanine aminotransferase (ALT), aspartate aminotransferase (AST), and lactate dehydrogenase (LDH), were all weakened, which clearly suggests that the NLRP3 inflammasome causes liver inflammation and damage. After the administration of MSNs, cellular ROS significantly increased, suggesting that ROS were involved in MSN-induced hepatotoxicity (Figure 7a, III). This research offers insights into the liver damage caused by MSNs and its mechanism and can help to increase the biological safety of MSNs.

### 3.2. Metal Oxide Nanoparticles

The liver and the mononuclear phagocyte system are common targets for designed nanoparticles. Therefore, it is crucial to conduct security assessments to evaluate interactions between MO<sub>x</sub> nanoparticles and phagocytic cells (or hepatocytes) of the liver. Nel et al. selected a broad array of MO<sub>x</sub> nanoparticles (29 nanoparticles), including REOs and transition-metal oxides (TMOs) to assess their toxicological profiles in primary and transformed KCs, macrophages, and hepatocytes (Figure 7b, I).<sup>[41]</sup> REOs (except CeO<sub>2</sub>) activated caspase-1 in KUP5 cells, whereas Hepa 1–6 cells did not behave in a similar way. Furthermore, a series of REOs and TMOs could trigger the activation of caspase-3 and -7 in KUP5 cells and Hepa 1–6 cells (Figure 7b, II). This suggests

that different cell uptake processes may lead to different cell death pathways. After siRNA knockdown of GSDMD, the LDH release from KUP5 cells which were cultured with CeO<sub>2</sub>, Gd<sub>2</sub>O<sub>3</sub>, La<sub>2</sub>O<sub>3</sub>, Y<sub>2</sub>O<sub>3</sub>, or Co<sub>3</sub>O<sub>4</sub> apparently decreased (Figure 7b, III), which indicates that REOs induced pyroptosis in KUP5 cells. Cellular responses of REOs were also studied in different cell types, such as primary KCs, BMDM, J774A.1, and RAW 264.7 cells, and it was found that pyroptosis was a specific characteristic for phagocytic cells but not for primary hepatocytes. This study establishes a small toxicological database which can help to provide toxicological information for security evaluation and risk analysis for toxins with similar structures.

The toxicity assessment of indium-tin-oxide (ITO) is of particular importance because workers who are in close contact with indium compounds have a significant risk of pulmonary alveolar proteinosis and interstitial lung disease. Nevertheless, the nosogenesis of these diseases is unknown. Suganuma et al. discovered the pathogenesis of respiratory illnesses induced by ITO and developed a strategy for the treatment of related diseases.<sup>[42]</sup> After intraperitoneal inoculation with ITO nanoparticles, the level of IL-1 $\beta$  within the peritoneal fluid was significantly increased, which indicated that ITO nanoparticles caused NLRP3 inflammasomes to exacerbate inflammation in mice. The size of endosomes in MH-S cells containing ITO nanoparticles was time- and dose-dependent (Figure 8a, I). Furthermore, the treated MH-S cells secreted TNF- $\alpha$ , suggesting that ITO nanoparticles induced the production of de novo protein. The exposure of <sup>51</sup>Cr-labeled MH-S cells to ITO nanoparticles could pump

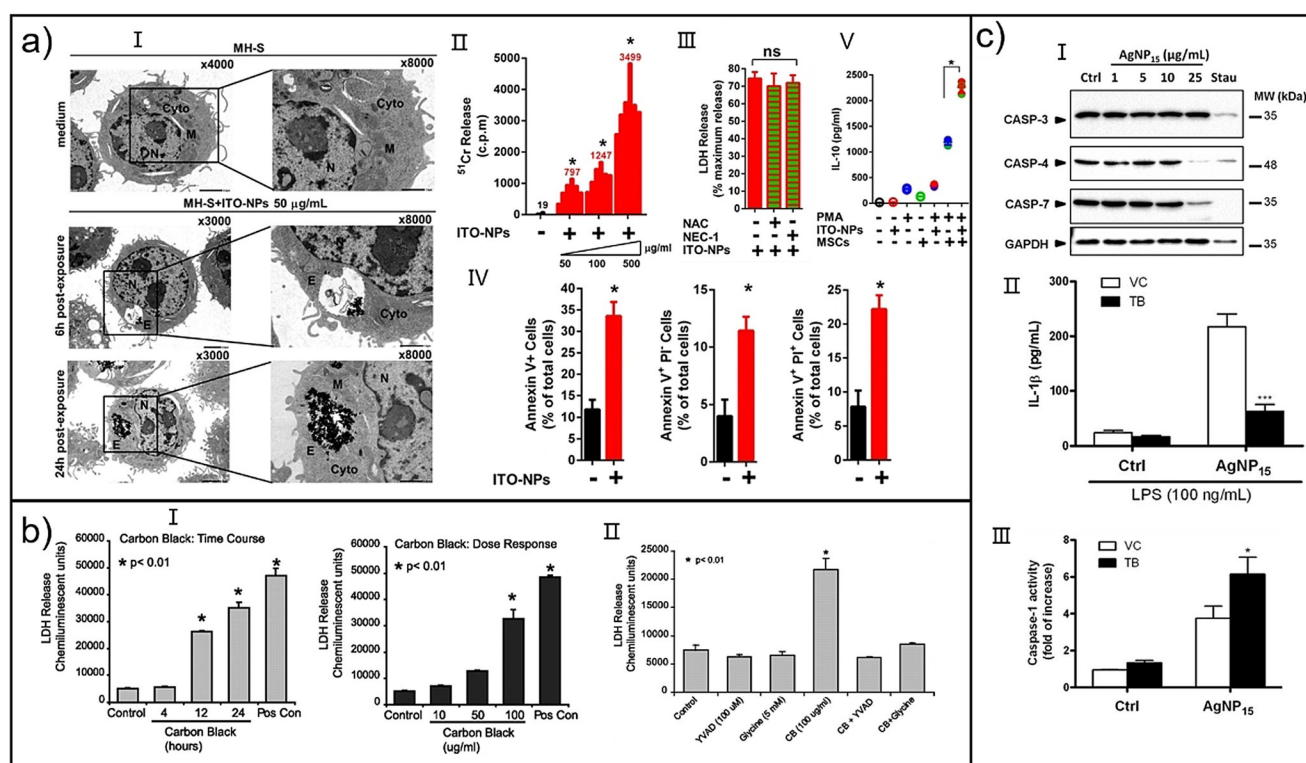


**Figure 8.** a) Effect of ITO nanoparticles on MH-S cells. I) Top: TEM of normal MH-S cells. Bottom: TEM of MH-S cells exposed to ITO nanoparticles. II) Release of  $^{51}\text{Cr}$  from MH-S cells upon exposure to different ITO nanoparticles. III) LDH release from MH-S cells after exposure to NAC, NEC-1, or ITO nanoparticles. IV) Percentage of differently stained cells after exposure to ITO nanoparticles, including Annexin V $^{+}$ , Annexin V $^{+}$ PI $^{-}$  or Annexin V $^{+}$ PI $^{+}$  cells. V) IL-10 release behavior after different treatments. b) Effect of CB on RAW164.7 cells. I) LDH release behavior of RAW164.7 cells after different treatments. II) LDH release behavior of RAW164.7 cells after different treatments. c) Effect of AgNP $_{15}$  on THP-1 cells. I) Caspase expression of human monocyte THP-1 cells after different treatments. II) IL-1 $\beta$  quantification of human monocyte THP-1 cells after different treatments. III) Caspase-1 activity assay of human monocyte THP-1 cells after different treatments. Reproduced with permission from Ref. [42]. Copyright 2016, Nature. Reproduced with permission from Ref. [43]. Copyright 2011, The American Society for Biochemistry and Molecular Biology. Reproduced with permission from Ref. [44]. Copyright 2011, The American Society for Biochemistry and Molecular Biology.

$^{51}\text{Cr}$  out of the cell (Figure 8a, II). In contrast, Ac-YVAD (caspase-1 inhibitor) significantly reduced  $^{51}\text{Cr}$  release. This shows that alveolar macrophages (AMs) treated with ITO nanoparticles experience a PCD which induces the rupture of the plasma membrane and is dependent on caspase-1. A LDH release assay demonstrated that the PCD was neither an apoptosis nor a necroptosis (Figure 8a, III), but a pyroptosis (Figure 8a, IV). Hence, pyroptosis was caspase-1-dependent, followed by plasma-membrane rupture and release of intracellular content. Lastly, it was observed that mesenchymal stem cells (MSCs) could protect macrophages from proinflammatory pyroptosis induced by ITO nanoparticles and might promote tissue regeneration and tissue healing by increasing IL-10 secretion (Figure 8a, V).

### 3.3. Carbon Black Nanoparticles

Inhalation of nanoparticles has been considered to be involved in respiratory diseases. Carbon black (CB) nanoparticles are discovered in many disparate environment exposures. Inhaled nanoparticles trigger macrophages to release inflammatory mediators and sometimes cell death.

As an important component in ambient pollution and an ingredient of toners in printers, carbon black nanoparticles are a pivotal target for toxicological assessment. CB nanoparticles could induce LDH release from RAW264.7 cells (Figure 8b, I), which shows that CB nanoparticles reduce the integrity of the plasma membrane and eventually induce cell death. Both YVAD (caspase-1 inhibitor) and glycine (pyroptosis inhibitor) attenuated the release of LDH; this demonstrates that CB nanoparticles induce pyroptosis (Figure 8b, II). This verification of a pyroptosis induced by CB nanoparticles is of great significance for the toxicological assessment of the impact of carbon-based particles on human health.<sup>[43]</sup>

### 3.4. Silver Nanoparticles

Many studies warn of the toxic effect of a variety of nanoparticles, such as TiO $_2$ , ZnO, and silver nanoparticles (AgNPs). However, the potential toxicity of AgNPs to humans is not completely elucidated, and it is therefore extremely urgent to explore the mechanism of their toxicity at the molecular and cellular level. Girard et al. carried out

experiments which filled this knowledge gap.<sup>[44]</sup> 25  $\text{g mL}^{-1}$  AgNP<sub>15</sub> (silver nanoparticles 15 nm in diameter) induced a quick degradation of activating transcription factor 6 (ATF-6), suggesting that AgNP<sub>15</sub> induced endoplasmic reticulum (ER) stress-dependent incidents in THP-1 cells. AgNP<sub>15</sub> (25  $\text{g mL}^{-1}$ ) affected the activation of caspase-4 and caspase-7, but not of caspase-3 (Figure 8c, I), which indicated that AgNP<sub>15</sub>-induced cell death was distinct from apoptosis. After siRNA (targeting NLRP-3) transfection, NLRP-3 protein expression and IL-1 secretion were markedly weakened. However, caspase-4 was demonstrated to be crucial for pro-IL-1, while its activity was independent of caspase-1 activation (Figure 8c, II and III). Inhibition of ATF-6 processing reduced caspase-1 processing and activation, the number of PI-positive cells, and IL-1 secretion; this demonstrates that the degradation of ATF-6 depends on the activity of the NLRP-3 inflammasomes and pyroptosis. In brief, AgNP<sub>15</sub> were able to trigger the decomposition of ATF-6, followed by the activation of the NLRP-3 inflammasome, which was adjusted by caspase-4 in THP-1 cells.

#### 4. Conclusion and Perspectives

The pyroptosis pathway is a new PCD variant that is regulated by the members of the gasdermin family and in which inflammasomes play a significant role. Although pyroptosis has recently been studied extensively in various inflammatory diseases, the understanding of the complex molecular mechanism of pyroptosis and its application in cancer research are still at an early stage. In an evaluation of previous research, we found only few contributions in which considerable efforts were focused on the cancer-specific mechanisms underlying the regulation of pyroptosis. Therefore, a considerable amount of work will need to be done to realize a cancer-selective therapy of pyroptosis. It is well known that drug resistance to apoptosis leads to the failure in the treatment of some refractory cancers. As a result, introduction of pyroptosis, which is a non-apoptotic PCD, may be a valid way to treat apoptosis-resistant cancers. It should be noted that pyroptosis may cause damage to normal cells and may build a microenvironment fit for tumor development and metastasis. This means that pyroptosis has a dual mechanism of inhibition and promotion of tumorigenesis and we should strictly use this double-edged sword to treat cancer.

At the moment, the most frequently used reagents to trigger pyroptosis of tumor cells are small molecules. Although small molecules have played significant roles in the therapy of cancers that are difficult to treat, they have several limitations including rapid clearance, systemic adverse reactions, and low accumulation at the tumor site. Benefiting from the progress in nanotechnology, the advantages of nanomaterials may compensate the limitations of pyroptotic reagents. Except for traditional passive targeting based on the EPR effect and active targeting using biological ligands, incorporation of stimuli-responsiveness in the nanoformulations to the tumor microenvironment is considered a novel therapeutic advantage to specifically kill cancer cells by

pyroptosis. As reported, the tumor microenvironment possesses some distinct physiological features, such as low pH, upregulated enzymes, and hypoxia. Stimuli-responsive nanoparticles which can be activated by the tumor microenvironment are able to selectively release drugs at the tumor site, thus enhancing cellular internalization and effectively promoting medicine perfusion throughout the solid tumor. The unwanted damage to normal organs/tissues can be avoided to a great extent by selectively activating pyroptosis in cancer cells through these sophisticated designs. However, there are still several problems which need to be addressed. For example, because of the diversity and heterogeneity of tumors, the differences of enzymatic activity or acidity between tumor and normal tissues are marginal; hence, there is an urgent need to design ultrasensitive nanomedicines which can be activated within a very narrow threshold. In addition, hypoxic regions are usually distant from blood vessels and it is therefore difficult for most nanomedicines to reach these regions. Nanomedicines that can release hypoxia-responsive prodrugs within tumor microenvironments will be a promising direction owing to a faster diffusion rate of small molecules. In order to avoid the undesirable cytotoxicity against normal organs caused by the nanocarriers, protective shells that are responsive to the tumor microenvironment can be introduced to improve their stability in normal tissues. When these smart nanomedicines reach the tumor, the stimuli-responsive shells can be removed inside the tumor and the pyroptosis process is initiated in the presence of these nanoformulations, which eventually leads to cell death and lysis. With respect to the application of various nanoparticles, the limitations of complex synthetic processes and colloidal instability during blood circulation are the major issues. Because of their dynamic nature, the construction of versatile supramolecular nanomaterials is easily possible by programmable self-assembly, which averts time-consuming preparation and purification processes.<sup>[45]</sup> The association constants between matching groups are relatively high, which guarantees that the complex will not disassemble after drug administration. Hence, supramolecular nanomaterials may provide a highly effective approach for potential pyroptosis-based cancer therapy.

The hypermethylation of GSDME mRNA in tumor cells leads to a low level of GSDME, which makes the initiation of pyroptosis more difficult in most tumor cells. Synergistic treatment involving demethylating drugs which can upregulate the level of GSDME expression is able to enhance the sensitivity of chemotherapeutic drugs and to reduce drug resistance. Other undefined gasdermin family proteins may also be closely associated with tumor inhibition and may offer new directions for the therapy of cancers. Owing to the existence of immune suppressor cells in the tumor microenvironment, systemic immune responses of most tumors are downregulated or inhibited. Being able to release proinflammatory intracellular contents, pyroptosis is a good opportunity for tumor immunotherapy. The activation of diversiform signaling pathways along with chemotherapeutic drugs used to enhance the systemic immune response would also be an effective method for cancer pathogenesis. The role of pyroptosis in cancer studies is just beginning to be under-

stood. With the increasingly better understanding of its mechanism, pyroptosis shows great potential for its comprehensive use in cancer diagnosis and treatment systems to benefit patients in the near future.

With the rapid development of society, a large number of nanomaterials have a great impact on our daily life and improve our work efficiency and quality of life. However, at the same time, frequent and heavy use of these nanomaterials is threatening our safety. For example, widely used MSNs can cause liver injury mediated by pyroptotic cell death; ITO nanoparticles can lead to occupational diseases with high mortality, such as pulmonary alveolar proteinosis and interstitial lung disease; AgNP<sub>15</sub> is able to trigger the decomposition of ATF-6, followed by NLRP-3 inflammasome activation, and eventually induce pyroptosis of normal cells. Therefore, it is high time to emphasize the importance of safety assessments of nanomaterials. The best way to avoid the harmful effects of nanomaterials is to build a powerful toxicity database which can provide sophisticated toxicology data for people who need it and lay down safety regulations for nanomaterials industries to minimize the occurrence of occupational diseases. We will hopefully enjoy the convenience brought by nanomaterials more safely in the near future.

### Acknowledgements

This work was supported by the Zhejiang Provincial Natural Science Foundation of China (LQ20B040001) and the Intramural Research Program, National Institute of Biomedical Imaging and Bioengineering, National Institutes of Health.

### Conflict of interest

The authors declare no conflict of interest.

- [1] a) F. Bray, A. Jemal, N. Grey, J. Ferlay, D. Forman, *Lancet Oncol.* **2012**, *13*, 790–801; b) D. S. Dizon, L. Krilov, E. Cohen, T. Gangadhar, P. A. Ganz, T. A. Hensing, S. Hunger, S. S. Krishnamurthi, A. B. Lassman, M. J. Markham, E. Mayer, M. Neuss, S. K. Pal, L. C. Richardson, R. Schilsky, G. K. Schwartz, D. R. Spriggs, M. A. Villalona-Calero, G. Villani, G. Masters, *J. Clin. Oncol.* **2016**, *34*, 987–1011.
- [2] a) H. Okada, T. W. Mak, *Nat. Rev. Cancer* **2004**, *4*, 592–603; b) C. Holohan, S. V. Schaeybroeck, D. B. Longley, P. G. Johnston, *Nat. Rev. Cancer* **2013**, *13*, 714–726; c) Z. Su, Z. Yang, L. Xie, J. P. DeWitt, Y. Chen, *Cell Death Differ.* **2016**, *23*, 748–756.
- [3] a) I. Bohm, H. Schild, *Mol. Imaging Biol.* **2003**, *5*, 2–14; b) V. Nikolettou, M. Markaki, K. Palikaras, N. Tavernarakis, *Biochim. Biophys. Acta.* **2013**, *1833*, 3448–3459; c) C. Y. Taabazuing, M. C. Okondo, D. A. Bachovchin, *Cell Chem. Biol.* **2017**, *24*, 507–514.
- [4] a) S. Doll, B. Proneth, Y. Y. Tyurina, E. Panzilius, S. Kobayashi, I. Ingold, M. Irmeler, J. Beckers, M. Aichler, A. Walch, H. Prokisch, D. Trümbach, G. Mao, F. Qu, H. Bayir, J. Füllekrug, C. H. Scheel, W. Wurst, J. A. Schick, V. E. Kagan, J. P. F. Angeli, M. Conrad, *Nat. Chem. Biol.* **2017**, *13*, 91–98; b) S. Neitemeier, A. Jelinek, V. Laino, L. Hoffmann, I. Eisenbach, R. Eying, G. K. Ganjam, A. M. Dolga, S. Oppermann, C. Culmsee, *Redox Biol.* **2017**, *12*, 558–570; c) M. Zille, S. S. Karuppagounder, Y. Chen, P. J. Gough, J. Bertin, J. Finger, T. A. Milner, E. A. Jonas, R. R. Ratan, *Stroke* **2017**, *48*, 1033–1043; d) B. Lu, X. Chen, M. Ying, Q. He, J. Cao, B. Yang, *Front. Pharmacol.* **2018**, *8*, 992.
- [5] A. Zychlinsky, M. C. Prevost, P. J. Sansonetti, *Nature* **1992**, *358*, 167–169.
- [6] a) H. Hilbi, Y. Chen, K. Thirumalai, A. Zychlinsky, *Infect. Immun.* **1997**, *65*, 5165–5170; b) D. Hersh, D. M. Monack, M. R. Smith, N. Ghorri, S. Falkow, A. Zychlinsky, *Proc. Natl. Acad. Sci. USA* **1999**, *96*, 2396–2401; c) B. T. Cookson, M. A. Brennan, *Trends Microbiol.* **2001**, *9*, 113–114.
- [7] a) J. Shi, Y. Zhao, K. Wang, X. Shi, Y. Wang, H. Huang, Y. Zhuang, T. Cai, F. Wang, F. Shao, *Nature* **2015**, *526*, 660–665; b) N. Kayagaki, I. B. Stowe, B. L. Lee, K. O'Rourke, K. Anderson, S. Warming, T. Cuellar, B. Haley, M. Roose-Girma, Q. T. Phung, P. S. Liu, J. R. Lill, H. Li, J. Wu, S. Kummerfeld, J. Zhang, W. P. Lee, S. J. Snipas, G. S. Salvesen, L. X. Morris, L. Fitzgerald, Y. Zhang, E. M. Bertram, C. C. Goodnow, V. M. Dixit, *Nature* **2015**, *526*, 666–671.
- [8] a) Y. Wang, W. Gao, X. Shi, J. Ding, W. Liu, H. He, K. Wang, F. Shao, *Nature* **2017**, *547*, 99–103; b) C. Rogers, T. Fernandes-Alnemri, L. Mayes, D. Alnemri, G. Cingolani, E. S. Alnemri, *Nat. Commun.* **2017**, *8*, 14128; c) P. Orning, D. Weng, K. Starheim, D. Ratner, Z. Best, B. Lee, A. Brooks, S. Xia, H. Wu, M. A. Kelliher, S. B. Berger, P. J. Gough, J. Bertin, M. M. Proulx, J. D. Goguen, N. Kayagaki, K. A. Fitzgerald, E. Lien, *Science* **2018**, *362*, 1064–1069; d) J. Sarhan, B. C. Liu, H. I. Muendlein, P. Li, R. Nilson, A. Y. Tang, A. Rongvaux, S. C. Bunnell, F. Shao, D. R. Green, A. Poltorak, *Proc. Natl. Acad. Sci. USA* **2018**, *115*, E10888–E10897; e) K. W. Chen, B. Demarco, R. Heilig, K. Shkarina, A. Boettcher, C. J. Farady, P. Pelczar, P. Broz, *EMBO J.* **2019**, *38*, e101638.
- [9] a) J. Shi, W. Gao, F. Shao, *Trends Biochem. Sci.* **2017**, *42*, 245–254; b) S. B. Kovacs, E. A. Miao, *Trends Cell Biol.* **2017**, *27*, 673–684; c) R. A. Aglietti, E. C. Duerber, *Trends Immunol.* **2017**, *38*, 261–271; d) X. Xia, X. Wang, Z. Cheng, W. Qin, L. Lei, J. Jiang, J. Hu, *Cell Death Dis.* **2019**, *10*, 650; e) S. Xia, L. R. Hollingsworth IV, H. Wu, *Cold Spring Harbor Perspect. Biol.* **2020**, *12*, a036400.
- [10] T. Bergsbaken, S. L. Fink, B. T. Cookson, *Nat. Rev. Microbiol.* **2009**, *7*, 99–109.
- [11] a) C. Rébé, V. Derangère, F. Ghiringhelli, *Mol. Cell. Oncol.* **2015**, *2*, e970094; b) I. Jorgensen, M. Rayamajhi, E. A. Miao, *Nat. Rev. Immunol.* **2017**, *17*, 151–164.
- [12] P. Broz, V. M. Dixit, *Nat. Rev. Immunol.* **2016**, *16*, 407–420.
- [13] a) M. Lamkanfi, V. M. Dixit, *Cell* **2014**, *157*, 1013–1022; b) S. K. Vanaja, V. A. K. Rathinam, K. A. Fitzgerald, *Trends Cell Biol.* **2015**, *25*, 308–315.
- [14] E. A. Miao, D. P. Mao, N. Yudkovsky, R. Bonneau, C. G. Lorang, S. E. Warren, I. A. Leaf, A. Aderem, *Proc. Natl. Acad. Sci. USA* **2010**, *107*, 3076–3080.
- [15] V. Hornung, A. Ablasser, M. Charrel-Dennis, F. Bauernfeind, G. Horvath, D. R. Caffrey, E. Latz, K. A. Fitzgerald, *Nature* **2009**, *458*, 514–516.
- [16] D. Boucher, M. Monteleone, R. C. Coll, K. W. Chen, C. M. Ross, J. L. Teo, G. A. Gomez, C. L. Holley, D. Bierschenk, K. J. Stacey, A. S. Yap, J. S. Bezbradica, K. Schroder, *J. Exp. Med.* **2018**, *215*, 827–840.
- [17] a) X. Liu, Z. Zhang, J. Ruan, Y. Pan, V. G. Magupalli, H. Wu, J. Lieberman, *Nature* **2016**, *535*, 153–158; b) J. Ding, K. Wang, W. Liu, Y. She, Q. Sun, J. Shi, H. Sun, D.-C. Wang, F. Shao, *Nature* **2016**, *535*, 111–116.
- [18] a) N. Kayagaki, S. Warming, M. Lamkanfi, V. L. Walle, S. Louie, J. Dong, K. Newton, Y. Qu, J. Liu, S. Heldens, J. Zhang, W. P. Lee, M. Roose-Girma, V. M. Dixit, *Nature* **2011**, *479*, 117–121; b) J. Shi, Y. Zhao, Y. Wang, W. Gao, J. Ding, P. Li, L. Hu, F. Shao, *Nature* **2014**, *514*, 187–192.

- [19] B. Zhou, J.-Y. Zhang, X.-S. Liu, H.-Z. Chen, Y.-L. Ai, K. Cheng, R.-Y. Sun, D. Zhou, J. Han, Q. Wu, *Cell Res.* **2018**, *28*, 1171–1185.
- [20] L. Wang, K. Li, X. Lin, Z. Yao, S. Wang, X. Xiong, Z. Ning, J. Wang, X. Xu, Y. Jiang, D. Liu, Y. Chen, D. Zhang, H. Zhang, *Cancer Lett.* **2019**, *450*, 22–31.
- [21] N. Pizato, B. C. Luzete, L. F. M. V. Kiffer, L. H. Corrêa, I. de Oliveira Santos, J. A. F. Assumpção, M. K. Ito, K. G. Magalhães, *Sci. Rep.* **2018**, *8*, 1952.
- [22] C.-C. Zhang, C.-G. Li, Y.-F. Wang, L.-H. Xu, X.-H. He, Q.-Z. Zeng, C.-Y. Zeng, F.-Y. Mai, B. Hu, D.-Y. Ouyang, *Apoptosis* **2019**, *24*, 312–325.
- [23] M. Wu, Y. Wang, D. Yang, Y. Gong, F. Rao, R. Liu, Y. Danna, J. Li, J. Fan, J. Chen, W. Zhang, Q. Zhan, *EBioMedicine* **2019**, *41*, 244–255.
- [24] P. Yu, H.-Y. Wang, M. Tian, A.-X. Li, X.-S. Chen, X.-L. Wang, Y. Zhang, Y. Cheng, *Acta Pharmacol. Sin.* **2019**, *40*, 1237–1244.
- [25] K. Strebhardt, A. Ullrich, *Nat. Rev. Cancer* **2008**, *8*, 473–480.
- [26] a) M. E. Davis, J. E. Zuckerman, C. H. J. Choi, D. Seligson, A. Tolcher, C. A. Alabi, Y. Yen, J. D. Heidel, A. Ribas, *Nature* **2010**, *464*, 1067–1070; b) J. Taberner, G. I. Shapiro, P. M. LoRusso, A. Cervantes, G. K. Schwartz, G. J. Weiss, L. Paz-Ares, D. C. Cho, J. R. Infante, M. Alsina, M. M. Gounder, R. Falzone, J. Harrop, A. C. S. White, I. Toudjarska, D. Bumcrot, R. E. Meyers, G. Hinkle, N. Svrzikapa, R. M. Hutabarat, V. A. Clausen, J. Cehelsky, S. V. Nocher, C. Gamba-Vitalo, A. K. Vaishnav, D. W. Y. Sah, J. A. Gollub, H. A. Burris III, *Cancer Discovery* **2013**, *3*, 406–417; c) J. Hrkach, D. Von Hoff, M. M. Ali, E. Andrianova, J. Auer, T. Campbell, D. De Witt, M. Figa, M. Figueiredo, A. Horhota, S. Low, K. McDonnell, E. Peeke, B. Retnajaran, A. Sabnis, E. Schnipper, J. J. Song, Y. H. Song, J. Summa, D. Tompsett, G. Troiano, T. Van Geen Hoven, J. Wright, P. LoRusso, P. W. Kantoff, N. H. Bander, C. Sweeney, O. C. Farokhzad, R. Langer, S. Zale, *Sci. Transl. Med.* **2012**, *4*, 128ra39.
- [27] a) Z. Shen, H. Wu, S. Yang, X. Ma, Z. Li, M. Tan, A. Wu, *Biomaterials* **2015**, *70*, 1–11; b) R. Bazak, M. Hourri, S. E. Achy, W. Hussein, T. Refaat, *Mol. Clin. Oncol.* **2014**, *2*, 904–908.
- [28] a) L. Wang, L.-L. Li, Y.-S. Fan, H. Wang, *Adv. Mater.* **2013**, *25*, 3888–3898; b) R. Dong, Y. Zhou, X. Huang, X. Zhu, Y. Lu, J. Shen, *Adv. Mater.* **2015**, *27*, 498–526; c) C. Chu, H. Lin, H. Liu, X. Wang, J. Wang, P. Zhang, H. Gao, C. Huang, Y. Zeng, Y. Tan, G. Liu, X. Chen, *Adv. Mater.* **2017**, *29*, 1605928; d) G. Yu, Z. Yang, X. Fu, B. C. Yung, J. Yang, Z. Mao, L. Shao, B. Hua, Y. Liu, F. Zhang, Q. Fan, S. Wang, O. Jacobson, A. Jin, C. Gao, X. Tang, F. Huang, X. Chen, *Nat. Commun.* **2018**, *9*, 766; e) G. Yu, X. Zhao, J. Zhou, Z. Mao, X. Huang, Z. Wang, B. Hua, Y. Liu, F. Zhang, Z. He, O. Jacobson, C. Gao, W. Wang, C. Yu, X. Zhu, F. Huang, X. Chen, *J. Am. Chem. Soc.* **2018**, *140*, 8005–8019.
- [29] J.-X. Fan, R.-H. Deng, H. Wang, X.-H. Liu, X.-N. Wang, R. Qin, X. Jin, T.-R. Lei, D. Zheng, P.-H. Zhou, Y. Sun, X.-Z. Zhang, *Nano Lett.* **2019**, *19*, 8049–8058.
- [30] P. Zhao, M. Wang, M. Chen, Z. Chen, X. Peng, F. Zhou, J. Song, J. Qu, *Biomaterials* **2020**, *254*, 120142.
- [31] a) W. Fan, N. Lu, P. Huang, Y. Liu, Z. Yang, S. Wang, G. Yu, Y. Liu, J. Hu, Q. He, J. Qu, T. Wang, X. Chen, *Angew. Chem. Int. Ed.* **2017**, *56*, 1229–1233; *Angew. Chem.* **2017**, *129*, 1249–1253; b) J. Li, Y. Li, Y. Wang, W. Ke, W. Chen, W. Wang, Z. Ge, *Nano Lett.* **2017**, *17*, 6983–6990; c) J. Li, A. Dirisala, Z. Ge, Y. Wang, W. Yin, W. Ke, K. Toh, J. Xie, Y. Matsumoto, Y. Anraku, K. Osada, K. Kataoka, *Angew. Chem. Int. Ed.* **2017**, *56*, 14025–14030; *Angew. Chem.* **2017**, *129*, 14213–14218.
- [32] J. Li, Y. Anraku, K. Kataoka, *Angew. Chem. Int. Ed.* **2020**, *59*, 13526–13530; *Angew. Chem.* **2020**, *132*, 13628–13632.
- [33] J. Hu, Y. Dong, L. Ding, Y. Dong, Z. Wu, W. Wang, M. Shen, Y. Duan, *Signal Transduct. Target. Ther.* **2019**, *4*, 28.
- [34] P. Clerc, P. Jeanjean, N. Hallali, M. Gougeon, B. Pipy, J. Carrey, D. Fourmy, V. Gigoux, *J. Controlled Release* **2018**, *270*, 120–134.
- [35] E. Ploetz, A. Zimpel, V. Cauda, D. Bauer, D. C. Lamb, C. Haisch, S. Zahler, A. M. Vollmar, S. Wuttke, H. Engelke, *Adv. Mater.* **2020**, *32*, 1907267.
- [36] Y. J. Choi, W. J. Chang, S. W. Shin, K. H. Park, S. T. Kim, Y. H. Kim, *Onco Targets Ther.* **2019**, *6*, 3307–3312.
- [37] N. Serna, P. Álamo, P. Rameshe, D. Vinokurova, L. Sánchez-García, U. Unzueta, A. Gallardo, M. V. Céspedes, E. Vázquez, A. Villaverde, R. Mangues, J. P. Medema, *J. Controlled Release* **2020**, *320*, 96–104.
- [38] Q. Wang, Y. Wang, J. Ding, C. Wang, X. Zhou, W. Gao, H. Huang, F. Shao, Z. Liu, *Nature* **2020**, *579*, 421–426.
- [39] D. L. Elion, M. E. Jacobson, D. J. Hicks, B. Rahman, V. Sanchez, P. I. Gonzales-Ericsson, O. Fedorova, A. M. Pyle, J. T. Wilson, R. S. Cook, *Cancer Res.* **2018**, *78*, 6183–6195.
- [40] X. Zhang, J. Luan, W. Chen, J. Fan, Y. Nan, Y. Wang, Y. Liang, G. Meng, D. Ju, *Nanoscale* **2018**, *10*, 9141–9152.
- [41] V. Mirshafiee, B. Sun, C. H. Chang, Y.-P. Liao, W. Jiang, J. Jiang, X. Liu, X. Wang, T. Xia, A. E. Nel, *ACS Nano* **2018**, *12*, 3836–3852.
- [42] A. Naji, B. A. Muzembo, K.-I. Yagy, N. Baba, F. Deschaseaux, L. Sensebé, N. Sukanuma, *Sci. Rep.* **2016**, *6*, 26162.
- [43] A. C. Reissetter, L. V. Stebounova, J. Baltrusaitis, L. Powers, A. Gupta, V. H. Grassian, M. M. Monick, *J. Biol. Chem.* **2011**, *286*, 21844–21852.
- [44] J.-C. Simard, F. Vallieres, R. de Liz, V. Lavastre, D. Girard, *J. Biol. Chem.* **2015**, *290*, 5926–5239.
- [45] a) D. Wu, Y. Li, J. Yang, J. Shen, J. Zhou, Q. Hu, G. Yu, G. Tang, X. Chen, *ACS Appl. Mater. Interfaces* **2017**, *9*, 44392–44401; b) J. Zhou, G. Yu, F. Huang, *Chem. Soc. Rev.* **2017**, *46*, 7021–7053; c) X. Li, E.-Y. Park, Y. Kang, N. Kwon, M. Yang, S. Lee, W. J. Kim, C. Kim, J. Yoon, *Angew. Chem. Int. Ed.* **2020**, *59*, 8630–8634; *Angew. Chem.* **2020**, *132*, 8708–8712; d) C. Chen, X. Ni, H.-W. Tian, Q. Liu, D.-S. Guo, D. Ding, *Angew. Chem. Int. Ed.* **2020**, *59*, 10008–10012; *Angew. Chem.* **2020**, *132*, 10094–10098; e) R. W. Chakraborty, A. Sneider, C. F. Anderson, F. Wang, P.-H. Wu, D. Wirtz, H. Cui, *Angew. Chem. Int. Ed.* **2020**, *59*, 4434–4442; *Angew. Chem.* **2020**, *132*, 4464–4472.

Manuscript received: July 27, 2020

Revised manuscript received: August 18, 2020

Accepted manuscript online: September 7, 2020

Version of record online: October 13, 2020